Received: 6 February 2023 | Revised: 6 June 2023 | Accepted: 4 July 2023

DOI: 10.1002/nme.7331

RESEARCH ARTICLE

WILEY

Eigensensitivity of damped system with distinct and repeated eigenvalues by chain rule

Ty Phuor[1,2] | **GilHo Yoon**[1]

[1]School of Mechanical Engineering, Hanyang University, Seoul, Republic of Korea

[2]Civil Engineering Department, Ariel University, Ariel, Israel

Correspondence
Ty Phuor, School of Mechanical Engineering, Hanyang University, Seoul 04763, Republic of Korea.
Email: ty168.utp@gmail.com

Funding information
National Research Foundation of Korea (NRF), Grant/Award Number: NRF_2019R1A2C2084974

Abstract

In this paper, a novel algorithm for computing the derivatives of eigensolutions of asymmetric damped systems with distinct and repeated eigenvalues is developed without using second-order derivatives of the eigenequations, which has a significant benefit over the existing published methods. To achieve this, the algorithm is proposed by (1) imposing consistent normalization conditions for both left and right eigenvectors throughout the computational system, and (2) solving sensitivity problems using the chain rule. These contributions add significant value to the proposed method. Additionally, the numerical difficulty is overcome by suggesting justifying Nelson (1976)'s technique based on the normalization conditions. Even though the proposed algorithm is simple and easy to implement, the employment of chain rule with new normalization in this note has never been reported in the literature, especially for the problem of eigensensitivity. Because this new algorithm does not require the second-order derivatives of the eigenequations, the analytical and numerical solutions for eigensensitivity offered by this method are less complicated than existing available solutions. The validity and applicability of the method are demonstrated through five numerical examples, showcasing its implementation in displacement- and state-space equations (rotordynamic system). Also, verifications are found to be in reasonable agreement with the approximated method.

KEYWORDS

asymmetric damped systems, chain rule, eigenvalue derivatives, eigenvector derivatives, Rotordynamic, sensitivity analysis

1 | INTRODUCTION

The solution of the eigenproblem sensitivities of the structural and mechanical systems with respect to structural design parameters plays an essential role in dynamic model updating, structural design optimization, structural dynamic modification, damage detection, model reanalysis, and many other applications.[1–3] For some specific systems, the derivative of the eigenvector may be computed with the eigenvector corresponding to distinct and/ or repeated eigenvalues, and the main difficulty in the computation is the singularity problem. Consequently, many computational techniques and methods have been developed to solve the eigensolution sensitivities of the systems with distinct and repeated eigenvalues.[1–7]

The first expression of the first-order derivatives of the eigensolution for the symmetric undamped system was given by Fox and Kapoor[8] by employing the modal expansion technique. Their method was extended to solve the sensitivity analysis of the asymmetric non-conservative systems by Rogers[9] and Plaut and Huseyin[10]; however, the latter method only adapted for the first-order representation of the equation of motion. Adhikari[11] produced the exact expression for the derivative of complex eigenvalues and eigenvectors of the second-order damped system. Later, with the classical normal modes, Adhikari[12] employed an approximated method to compute the derivative of complex modes for non-proportionally symmetric damped systems. Then, this method was extended to the first- and second-order derivatives of the eigensolutions of the asymmetric systems with viscous damping by Adhikari.[13] Similarly, Zeng[14] proposed the modified modal method for solving the complex eigenvectors in the symmetric damped systems and the extension of this modified method was then performed for the general asymmetric damped systems by Moon et al.[15] However, these methods were reported with less accuracy.[1]

Nelson[16] presented an efficient algorithm for calculating eigenvector derivatives with distinct eigenvalues for the self-adjoint asymmetric system by expressing the derivative of each eigenvector as a particular solution and a homogeneous solution. However, the weakness of Nelson's method was found with the repeated eigenvalue system; consequently, the extensions were conducted by many researchers (e.g., Mills-Curran,[17] Ojalvo,[18] Dailey[19]) to solve the derivatives of eigenvalues and eigenvectors of the real symmetric eigensystems with repeated eigenvalues. Later, the improvement was performed to compute the eigensolution derivatives in the case of repeated eigenvalues with the repeated first-order eigenvalue derivatives by Shaw and Jayasuriya.[20] Then, Tang et al.[21] and Tang and Wang[22] investigated the eigensolution derivatives with repeated eigenvalues for general asymmetric systems. Subsequently, Friswell and Adhikari[23] extended Nelson's method to symmetric and asymmetric systems with viscous damping. Similarly, Xu and Wu[2] developed a method to compute eigensolution derivatives of damped systems with distinct and repeated eigenvalues by imposing a new normalization condition. It is worth pointing out that the methods mentioned above belong to the Nelson-type method.

Besides, Lee et al.[24] proposed an iterative method, while Burchett and Costello[25] proposed a *QR*-based algorithm, which is a way to decompose a matrix into Q and R matrices, where Q is an orthogonal matrix and R is an upper triangle matrix, for sensitivity analysis of eigensystems with distinct and repeated eigenvalues. Xie and Dai[26] employed a Davidson method for solving the first-order eigensolution derivatives of the symmetric generalized eigenvalue problems. Lee[27] analyzed the design sensitivity of repeated eigenvalues and associated eigenvectors by suggesting the adjoint method, in which the computation of the adjoint variables from the simultaneous linear system equations could be performed without using the linear combination of the eigenvectors. Burchett[28] developed a computation technique in conjunction with the *QZ* algorithm, which is a method to find orthogonal matrices Q and Z. Thus, the derivatives of system poles and transmission zeros are computed simultaneously with the poles and zeros themselves. Recently, Yoon et al.[29] proposed a highly efficient general method for sensitivity analysis of eigenvectors with repeated eigenvalues for the symmetric system without passing through adjacent eigenvectors in calculating the partial derivatives of any prescribed eigenvector basis. However, these methods hardly solve the eigenproblem sensitivities for the non-self-adjoint asymmetric systems.

For solving the eigen derivatives, the linear system of algebraic equations is employed;[30–32] however, this method was only restricted to the first-order representation of the equation of motion.[1] Likewise, this method was also used with symmetric coefficient matrices for undamped systems with distinct[33] and repeated eigenvalues.[34] Later, their algebraic methods were extended to the second-order symmetric damped systems with distinct and repeated eigenvalues.[35,36] However, Wu et al.[37] reported that these methods (e.g., References 34,35) were not correct due to a mistake in the derivation of the normalization for solving the repeated eigenvalues.[1]

On the contrary, for the non-symmetric system, the algebraic methods were extended to the derivatives of eigenvalues and eigenvectors,[38] and a further extension was made by Chouchane et al.[39] to the second-order derivatives of the eigensolutions and reported that their method might compute the higher-order eigensolution derivatives. Later, Xu et al.[4] developed an efficient algebraic method to calculate the eigensolution derivatives of asymmetric damped systems by employing a new normalization and pointed out that their method was computationally more efficient than the method proposed by Reference 38. However, these methods[4,38,39] are limited to the case of distinct eigenvalues and additionally, because the components of the constraints and system matrices in the coefficient matrices are not all of the same order of magnitude, the algebraic method may be ill-conditioned.[1] Consequently, Li et al.[1] proposed an efficient method for computing the derivatives of the eigenvalues and associated eigenvectors of asymmetric damped systems with distinct and repeated eigenvalues by introducing a new additional normalization for the left eigenvectors. The authors reported that their methods are computationally efficient because the left and right eigenvector derivatives can be computed in a parallel way, and the components of coefficient matrices are all of the same order of magnitude. Wang and Dai[3] proposed the algorithm for computing the eigenpair derivatives of asymmetric quadratic eigenvalue

problems with distinct and repeated eigenvalues by imposing the additional normalization condition. It was reported that this method is numerically stable, and the homogenous solutions are computed by the second-order derivative of the eigenequations.

Likewise, Wang and Yang[6] developed a method for sensitivity calculation of defective repeated eigenpairs of the generalized eigenvalue and quadratic eigenproblems. They stated that the computed results are useful for investigating optimal structural design, model updating, and structural damage detection. Besides, Wang et al.[7] proposed another new algorithm for calculating the derivatives of the semisimple eigenvalues and corresponding eigenvectors of an asymmetric damped system, in which the eigenvectors derivatives are divided into a particular solution and a homogenous solution, where the particular solution is solved by employing the generalized inverse matrix. Later, Wang et al.[5] extended the method[7] for computing the eigenpair derivatives of the damped system by dividing it into a particular solution and a general solution of the corresponding homogenous equation. Despite the successful development of various techniques for computing derivatives of complex eigenvectors with distinct and repeated eigenvalues,[1–7] to the best of the authors' knowledge, there is still no report highlighting the most suitable method for practical design optimization of rotordynamic systems. Furthermore, when dealing with complex rotating structures, which involve components such as elastic, Coriolis, and centrifugal stiffness matrices, as well as mass, gyroscopic, and damping matrices, and so forth,[40] the existing methods may be costly and time-consuming to achieve design optimization objectives, such as maximizing critical speed, due to the tediousness and complexity of the employment of the second-order derivatives of the eigenequations and the inconsistent normalization condition (e.g., Reference 4). Consequently, a more simpler approach should be proposed.

Therefore, this paper presents a new algorithm for solving the derivatives of the eigensolutions corresponding to the distinct and repeated eigenvalues in an asymmetric damped system without utilizing the second-order derivatives of the eigenequations, which has a substantial advantage over the existing available methods. To accomplish this, the new algorithm is developed by (1) imposing simple normalization conditions for the left and right eigenvectors and making the conditions to be consistent in the entire computational system and (2) solving the sensitivity problems by using the chain rule. These contributions represent significant advancements in the field of the present method, distinguishing it from existing approaches where normalization conditions lack consistency during the computational procedure, as demonstrated in Reference 4. Notably, this new method offers an alternative to previous techniques by utilizing the chain rule, while eliminating the need for the second-order derivatives of the eigenequations, providing substantial benefits over existing solutions. Consequently, the present method is simpler and more straightforward to implement in analytical and numerical programs. In addition, numerical stability might be achieved by suggesting justifying Nelson[16] technique on the basis of the new normalizations. Importantly, the developed method presented herein is crucial for solving the derivatives of the critical speeds and the derivatives of the unbalanced responses to update and find the optimum solutions of the rotordynamic system, such as minimizing unwanted noise (level vibration), increasing the magnitude of the critical speeds of the rotating structures, and so forth. The proposed methodology for the sensitivity analysis of asymmetric damped systems is presented in Section 2. The numerical examples to illustrate the implementation and the validation of the proposed method; and the conclusion and recommendation for future work are presented in Sections 3 and 4, respectively.

2 | PROPOSED METHOD

The general equation of motion for free vibration of a linear damped system with n degrees of freedom is expressed by

$$M(q)\ddot{r}(t) + C(q)\dot{r}(t) + K(q)r(t) = 0 \tag{1}$$

where $M(q)$, $C(q)$ and $K(q) \in \mathbb{R}^{n\times n}$ are respectively the mass, damping, and stiffness matrices which are in function of the actual design variable q. $\ddot{r}(t)$, $\dot{r}(t)$ and $r(t)$ stand for the vector of acceleration, velocity, and displacement, and t denotes the time. It is noticed that the mass matrix is nonsingular, and the system matrices are nonsymmetric matrices. From Equation (1), the right and left eigenvectors can respectively be computed by Equations (2) and (3).[1–7]

$$\left(\lambda_i^2(q)M(q) + \lambda_i(q)C(q) + K(q)\right)\varphi_i(q) = 0, i = 1, 2, \ldots, n \tag{2a}$$

$$\left(\lambda_i^2(q)M(q) + \lambda_i(q)C(q) + K(q)\right)^T\psi_i(q) = 0, i = 1, 2, \ldots, n \tag{2b}$$

where $\varphi_i(q) \in \mathbb{C}^n$ and $\psi_i(q) \in \mathbb{C}^n$ are the i-th right and left eigenvectors. $\lambda_i(q) \in \mathbb{C}^n$ is the ith eigenvalue. The $2n$-dimensional first-order eigenvalue problem can also be obtained by transforming Equation (2) into the state-space equation.[2,40]

$$E(q)\eta_i(q) = \lambda_i(q)F(q)\eta_i(q), i = 1, 2, \ldots, n \tag{3a}$$

$$E^T(q)\xi_i(q) = \lambda_i(q)F^T(q)\xi_i(q), i = 1, 2, \ldots, n \tag{3b}$$

where, $E(q) = \begin{bmatrix} -K(q) & 0 \\ 0 & M(q) \end{bmatrix}, F(q) = \begin{bmatrix} C(q) & M(q) \\ M(q) & 0 \end{bmatrix}$

$$\eta_i(q) = \begin{Bmatrix} \varphi_i \\ \lambda_i\varphi_i \end{Bmatrix}, \xi_i(q) = \begin{Bmatrix} \psi_i \\ \lambda_i\psi_i \end{Bmatrix}$$

As the mass matrix is nonsingular, the normalization of the eigenvector of the state-space equation (Equation 3) and displacement-space equation (Equation 2) can be expressed as in Equations (4a) and (4b), respectively.

$$\xi_i^T(q)F(q)\eta_i(q) = 1, i = 1, 2, \ldots, n \tag{4a}$$

$$\psi_i^T(q)\left(2\lambda_i(q)M(q) + C(q)\right)\varphi_i(q) = 1, i = 1, 2, \ldots, n \tag{4b}$$

For solving the sensitivity analysis of the asymmetric system, it is well acknowledged that it is not sufficient to ensure the uniqueness of the eigenvector by employing the normalization in Equation (4). Obviously, Equation (4) is also satisfied, and it may be checked by multiplying the left eigenvectors by any nonzero scalar and dividing the right eigenvectors by the same scalar. Consequently, to guarantee the uniqueness of the eigensolutions in this paper, additional normalizations should be imposed, which are presented with the respective eigensolution derivatives.

2.1 | Eigensolution derivatives of repeated eigenvalue

The expressions of the eigenproblems are defined by

$$\left(\chi_m^2(q)M(q) + \chi_m(q)C(q) + K(q)\right)u_m(q) = 0 \tag{5}$$

$$\left(\chi_m^2(q)M(q) + \chi_m(q)C(q) + K(q)\right)^T v_m(q) = 0 \tag{6}$$

where,

$$\chi_m(q) = \lambda_m = \lambda_l I_m$$

$$u_m(q) = \left[\varphi_m^1(q) \quad \varphi_m^2(q) \quad \cdots \quad \varphi_m^m(q)\right]$$

$$v_m(q) = \left[\psi_m^1(q) \quad \psi_m^2(q) \quad \cdots \quad \psi_m^m(q)\right]$$

where $\chi_m(q)$ is the $(m \times m)$ matrix in which its diagonal contains the eigenvalue, I_m is the identity matrix of order m, and λ_l is the lth eigenvalue of multiplicity m $(1 < m \leq n)$ for the eigenspace spanned by the columns of $u_m(q)$ or $v_m(q)$. Similar to Equation (4), for $q = q_0$, the normalization of the eigenvectors at the lth eigenvalue can be written as

$$\left\{\psi_m^j\right\}^T \left(2\lambda_l M + C\right)\varphi_m^k = \delta_{jk} \tag{7}$$

where ψ_m^j and φ_m^k are respectively the left and right eigenvectors corresponding to the eigenvalue (λ_l). δ_{jk} is the Kronecker delta, where $\delta_{jk} = 1$ if $j = k$ and otherwise, $\delta_{jk} = 0$. From this concept, the orthogonal normalization for the u_m and v_m of

the m repeated eigenvalues can be expressed as

$$v_m^T \left(2\lambda_m M + C\right) u_m = I_m \tag{8}$$

2.1.1 | The eigenvalue sensitivity and adjacent eigenvectors

For the repeated eigenvalues, the derivative of the eigenvalue has to be computed directly by solving the eigenproblem, which contains the adjacent eigenvectors. Thus, the adjacent eigenvectors in terms of $u_m(q)$ and $v_m(q)$ can be expressed by

$$U_m(q) = u_m(q) \cdot \sigma \tag{9}$$

$$V_m(q) = v_m(q) \cdot \tau \tag{10}$$

where σ and τ are the $(m \times m)$ nonsingular transformation matrices. Consequently, the eigenproblems in Equations (5) and (6) become

$$\left(\chi_m^2(q)M(q) + \chi_m(q)C(q) + K(q)\right) U_m(q) = 0 \tag{11}$$

$$\left(\chi_m^2(q)M(q) + \chi_m(q)C(q) + K(q)\right)^T V_m(q) = 0 \tag{12}$$

Then, by applying the differentiation for $q = q_0$, Equation (11) becomes

$$\left(2\lambda_l M + C\right) U_m \frac{\partial \chi_m}{\partial q} = -\left(\lambda_l^2 M + \lambda_l C + K\right) \frac{\partial U_m}{\partial q} - \left(\lambda_l^2 \frac{\partial M}{\partial q} + \lambda_l \frac{\partial C}{\partial q} + \frac{\partial K}{\partial q}\right) U_m \tag{13}$$

By pre-multiplying both sides of Equation (13) with v_m^T and employing Equations (8)–(10), the derivative of the eigenvalue can be obtained by solving the right eigenvalue problem in Equation (14).

$$D \cdot \sigma = \sigma \cdot \frac{\partial \chi_m}{\partial q} \tag{14}$$

By following the same procedures for the left eigenvector, the eigenvalue derivative can also be computed by

$$D^T \cdot \tau = \tau \cdot \frac{\partial \chi_m}{\partial q} \tag{15}$$

where,

$$D = -v_m^T \left(\lambda_l^2 \frac{\partial M}{\partial q} + \lambda_l \frac{\partial C}{\partial q} + \frac{\partial K}{\partial q}\right) u_m \tag{16a}$$

By following the same arguments mentioned above, D can also be calculated in the state-space equation as in Equation (16b).

$$D = -vss_m^T \left(\lambda_l \frac{\partial E}{\partial q} - \frac{\partial F}{\partial q}\right) uss_m \tag{16b}$$

where $uss_m = u_m, vss_m = v_m$, if the displacement-space equation is considered.

It is worth mentioning that the derivatives of the eigenvalues can be achieved by the need of only the eigenvalue and associated eigenvectors and the derivatives of the system matrices. In addition, the σ and τ must be normalized in such a way that

$$V_m^T \left(2\lambda_m M + C\right) U_m = I_m, \text{for the displacement} - \text{space equation} \tag{17a}$$

$$Vss_m^T \cdot F \cdot Uss_m = I_m, \text{for the state} - \text{space equation} \tag{17b}$$

where, $Uss_m = uss_m \cdot \sigma$, $Vss_m = vss_m \cdot \tau$.

2.1.2 | The eigenvector sensitivity

From Equation (17), the normalization equation can also be $\tau^T\sigma = I_m$. However, this normalization is not sufficient to ensure the uniqueness of eigenvectors because the equation is still verified when multiplying σ by any nonzero scalar and dividing τ by the same scalar.[4] Therefore, to guarantee uniqueness, an additional normalization should be imposed for $q = q_0$ as in Equation (18).

$$\left\{U_j\right\}_i = 1 \; and \; \left\{V_j\right\}_i = 1, where \, j = 1, 2, \ldots, n \tag{18}$$

where $\left\{\blacksquare_j\right\}_i$ is the i^{th} component of the j^{th} eigenvector. The ith component is selected in such a way that the absolute value of the corresponding component in the eigenvector is the largest, as seen in Equation (19).

$$\left|\left\{U_j\right\}_i\right|\left|\left\{V_j\right\}_i\right| = \max_{k=1,2,\ldots,n}\left|\left\{U_j\right\}_k\right|\left|\left\{V_j\right\}_k\right| \tag{19}$$

Consequently, $\tilde{U}_m$ and $\tilde{V}_m$ denote the right and left eigenvectors after applying the normalization (Equation (18)). Then, in order to fulfill the normalization in Equation (17a), the final eigenvectors may be recalculated by

$$u_m = \frac{\tilde{U}_m}{\left(\tilde{V}_m^T\left(2\lambda_m M + C\right)\tilde{U}_m\right)^{1/2}} \; and \; v_m = \frac{\tilde{V}_m^T}{\left(\tilde{V}_m^T\left(2\lambda_m M + C\right)\tilde{U}_m\right)^{1/2}} \tag{20}$$

Similarly, in the state-space equation, the eigenvectors can be expressed as

$$uss_m = \frac{\tilde{U}ss_m}{\left(\tilde{V}ss_m^T \cdot F \cdot \tilde{U}ss_m\right)^{1/2}} \; and \; vss_m = \frac{\tilde{V}ss_m^T}{\left(\tilde{V}ss_m^T \cdot F \cdot \tilde{U}ss_m\right)^{1/2}} \tag{21}$$

Consequently, by employing Equation (13), the eigenvector derivative $\partial\tilde{U}_m/\partial q$ can be computed as in Equation (22a). Also, by applying similar arguments, the derivative of the left eigenvector $\partial\tilde{V}_m/\partial q$ is given as in Equation (22b).

$$B_m\frac{\partial\tilde{U}_m}{\partial q} = AU_m \tag{22a}$$

$$B_m^T\frac{\partial\tilde{V}_m}{\partial q} = AV_m \tag{22b}$$

where,

$$B_m = \lambda_m^2 M + \lambda_m C + K \tag{23}$$

$$AU_m = -\left(2\lambda_m M + C\right)\tilde{U}_m\frac{\partial\chi_m}{\partial q} - \left(\lambda_m^2\frac{\partial M}{\partial q} + \lambda_m\frac{\partial C}{\partial q} + \frac{\partial K}{\partial q}\right)\tilde{U}_m \tag{24}$$

$$AV_m = -\left(2\lambda_m M + C\right)^T\tilde{V}_m\frac{\partial\chi_m}{\partial q} - \left(\lambda_m^2\frac{\partial M}{\partial q} + \lambda_m\frac{\partial C}{\partial q} + \frac{\partial K}{\partial q}\right)^T\tilde{V}_m \tag{25}$$

Because B_m may be singular, Equation (22) is hardly solved. Consequently, Equation (22) can be solved by using Nelson[16] technique. Therefore, the right and left eigenvectors derivatives for the displacement-space equation can be computed using the chain rule as in Equations (26a) and (26b), respectively.

$$\frac{\partial u_m}{\partial q} = \frac{\partial u_m}{\partial \tilde{U}_m}\frac{\partial \tilde{U}_m}{\partial q} \tag{26a}$$

$$\frac{\partial v_m}{\partial q} = \frac{\partial v_m}{\partial \tilde{V}_m}\frac{\partial \tilde{V}_m}{\partial q} \tag{26b}$$

Using the same procedures, the derivative of the eigenvectors in the state-space equation can be expressed as in Equation (27).

$$\frac{\partial uss_m}{\partial q} = \frac{\partial uss_m}{\partial \tilde{U}ss_m}\frac{\partial \tilde{U}ss_m}{\partial q} \tag{27a}$$

$$\frac{\partial vss_m}{\partial q} = \frac{\partial vss_m}{\partial \tilde{V}ss_m}\frac{\partial \tilde{V}ss_m}{\partial q} \tag{27b}$$

2.2 | Eigensolution derivatives of distinct eigenvalue

When $m = 1$, the system is calculated with the distinct eigenvalue and by differentiating Equation (2) with respect to the design variable q for $q = q_0$, the differential equations of the right and left eigenvectors can be written as in Equations (28) and (29), respectively.

$$(2\lambda_i M + C)\,\varphi_i \frac{\partial \lambda_i}{\partial q} = -\left(\lambda_i^2 M + \lambda_i C + K\right)\frac{\partial \varphi_i}{\partial q} - \left(\lambda_i^2 \frac{\partial M}{\partial q} + \lambda_i \frac{\partial C}{\partial q} + \frac{\partial K}{\partial q}\right)\varphi_i \tag{28}$$

$$(2\lambda_i M + C)^T \psi_i \frac{\partial \lambda_i}{\partial q} = -\left(\lambda_i^2 M + \lambda_i C + K\right)^T \frac{\partial \psi_i}{\partial q} - \left(\lambda_i^2 \frac{\partial M}{\partial q} + \lambda_i \frac{\partial C}{\partial q} + \frac{\partial K}{\partial q}\right)^T \psi_i \tag{29}$$

By pre-multiplying both sides of Equation (28) with ψ_i^T and employing the normalization conditions Equations (3) and (4), the eigenvalue derivative of the distinct eigenvalue can be computed by

$$\frac{\partial \lambda_i}{\partial q} = -\psi_i^T \left(\lambda_i^2 \frac{\partial M}{\partial q} + \lambda_i \frac{\partial C}{\partial q} + \frac{\partial K}{\partial q}\right)\varphi_i \tag{30a}$$

With the same arguments, the eigenvalue derivative of the distinct eigenvalue in the state-space equation can be computed by

$$\frac{\partial \lambda_i}{\partial q} = -\xi_i^T \left(\lambda_i \frac{\partial E}{\partial q} - \frac{\partial F}{\partial q}\right)\eta_i \tag{30b}$$

As mentioned earlier, the normalization condition in Equation (4) is not sufficient. Therefore, an additional normalization should be imposed for $q = q_0$ as in Equation (31).

$$\left\{\varphi_j\right\}_i = 1 \; and \; \left\{\psi_j\right\}_i = 1, where \, j = 1, 2, \ldots, n \tag{31}$$

The ith component can be chosen in such a way that the absolute value of the corresponding component in the eigenvector is the largest, as in Equation (32).

$$\left|\left\{\varphi_j\right\}_i\right|\left|\left\{\psi_j\right\}_i\right| = \max_{k=1,2,\ldots,n}\left|\left\{\varphi_j\right\}_k\right|\left|\left\{\psi_j\right\}_k\right| \tag{32}$$

Consequently, $\tilde{\varphi}_j$ and $\tilde{\psi}_j$ denote the right and left eigenvectors after applying the normalization (Equation (31)). Then, in order to fulfill the normalization in Equation (4), the final eigenvectors may be recalculated by

$$\varphi_i = \frac{\tilde{\varphi}_i}{\left(\tilde{\psi}_i^T (2\lambda_i M + C)\,\tilde{\varphi}_i\right)^{1/2}} \; and \; \psi_i = \frac{\tilde{\psi}_i^T}{\left(\tilde{\psi}_i^T (2\lambda_i M + C)\,\tilde{\varphi}_i\right)^{1/2}} \tag{33}$$

Consequently, by employing Equations (28) and (29), the eigenvector derivatives $\partial\tilde{\varphi}_i/\partial q$ and $\partial\tilde{\psi}_i/\partial q$ can be computed as in Equations (34) and (35), respectively.

$$B_i\frac{\tilde{\varphi}_i}{\partial q} = AU_i \tag{34}$$

$$B_i^T\frac{\partial\tilde{\psi}_i}{\partial q} = AV_i \tag{35}$$

where,

$$B_i = \lambda_i^2 M + \lambda_i C + K \tag{36}$$

$$AU_i = -\left(2\lambda_i M + C\right)\tilde{\varphi}_i\frac{\partial\lambda_i}{\partial q} - \left(\lambda_i^2\frac{\partial M}{\partial q} + \lambda_i\frac{\partial C}{\partial q} + \frac{\partial K}{\partial q}\right)\tilde{\varphi}_i \tag{37}$$

$$AV_i = -(2\lambda_i M + C)^T\tilde{\psi}_i\frac{\partial\lambda_i}{\partial q} - \left(\lambda_i^2\frac{\partial M}{\partial q} + \lambda_i\frac{\partial C}{\partial q} + \frac{\partial K}{\partial q}\right)^T\tilde{\psi}_i \tag{38}$$

It is well known that Equations (34) and (35) are hardly solved due to the singularity problems. Consequently, by applying Nelson[16] technique, the eigenvector derivatives $\partial\tilde{\varphi}_i/\partial q$ and $\partial\tilde{\psi}_i/\partial q$ can be computed. Finally, the right and left eigenvectors derivatives in the displacement-space equation can be computed using the chain rule as in Equations (39a) and (39b), respectively.

$$\frac{\partial\varphi_i}{\partial q} = \frac{\partial\varphi_i}{\partial\tilde{\varphi}_i}\frac{\partial\tilde{\varphi}_i}{\partial q} \tag{39a}$$

$$\frac{\partial\psi_i}{\partial q} = \frac{\partial\psi_i}{\partial\tilde{\psi}_i}\frac{\partial\tilde{\psi}_i}{\partial q} \tag{39b}$$

Similarly, following the same procedures above, the right and left eigenvectors derivatives can also be computed in the state-space equation using the chain rule as Equations (40a) and (40b), respectively.

$$\frac{\partial\eta_i}{\partial q} = \frac{\partial\eta_i}{\partial\tilde{\eta}_i}\frac{\partial\tilde{\eta}_i}{\partial q} \tag{40a}$$

$$\frac{\partial\xi_i}{\partial q} = \frac{\partial\xi_i}{\partial\tilde{\xi}_i}\frac{\partial\tilde{\xi}_i}{\partial q} \tag{40b}$$

2.3 | Discussion on the numerical stability of the proposed method

In the existing methods (e.g., References 1–7), the derivative of the eigenvectors has been performed by using the linear combination of the eigenvectors. On the contrary, the proposed method in this note is carried out by employing the chain rule. More precisely, Figure 1 illustrates the diagram that compares the computation procedures produced by the existing methods and a newly proposed method in this paper. Moreover, it is worth noticing that the eigensolutions derivatives are derived from the proposed computational procedures, making the normalization conditions more consistent than the computational procedures employed by some researchers, for example, Xu et al.[4] These conditions are demonstrated and verified with the numerical examples provided in Section 3. Consequently, to the best of the authors' knowledge, the authors believe that this proposed computational method would provide reliable responses because the iterative loop work is required in design optimization. From a mathematical point of view, in the entire computational procedure of the proposed method, the numerical instability may occur at only the solution of the Equations (41a) and (41b) for the repeated eigenvalue and Equations (42a) and (42b) for the distinct eigenvalue.

$$\left(\lambda_m^2 M + \lambda_m C + K\right)\frac{\partial\tilde{U}_m}{\partial q} = -\left(2\lambda_m M + C\right)\tilde{U}_m\frac{\partial\chi_m}{\partial q} - \left(\lambda_m^2\frac{\partial M}{\partial q} + \lambda_m\frac{\partial C}{\partial q} + \frac{\partial K}{\partial q}\right)\tilde{U}_m \tag{41a}$$

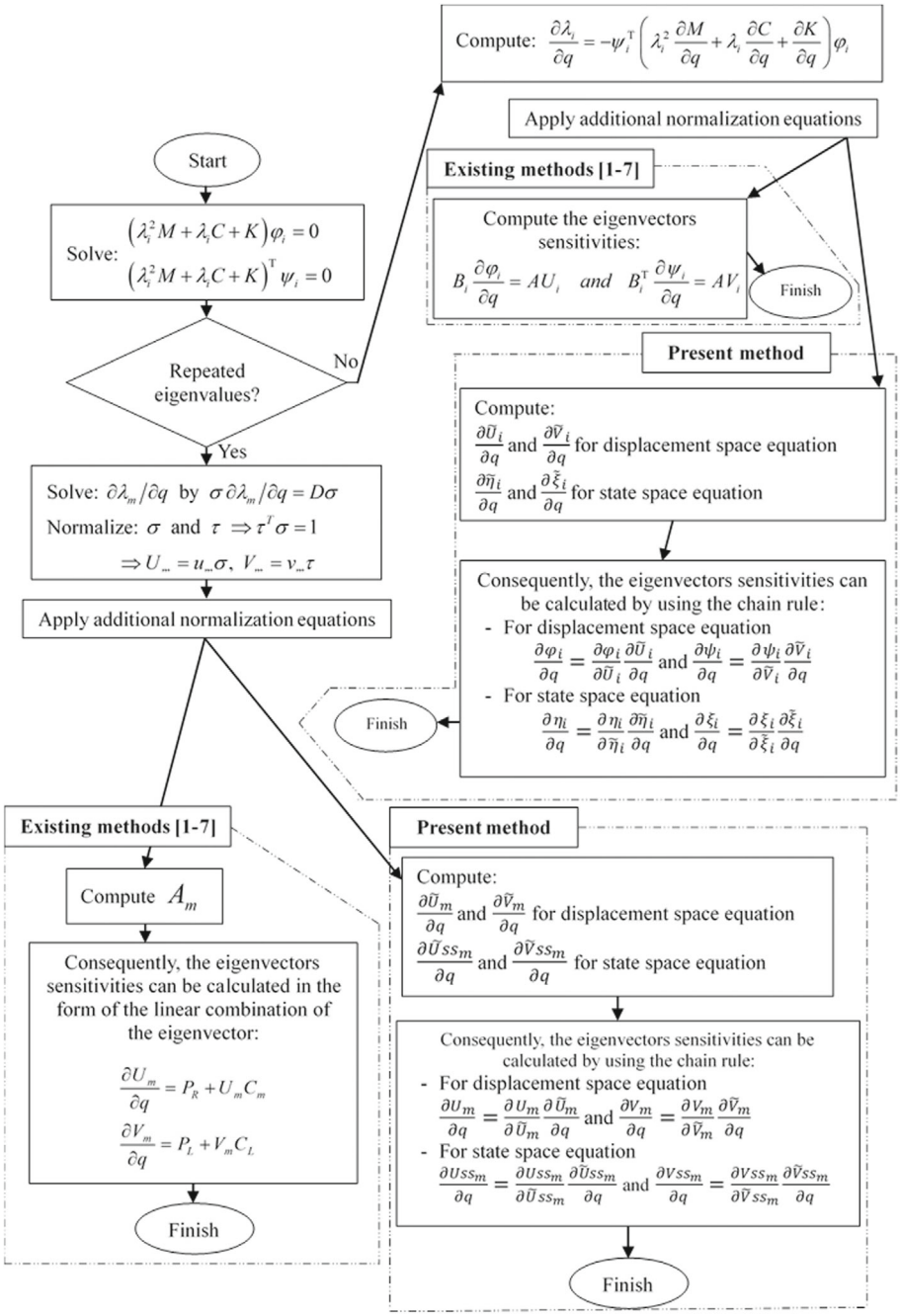

FIGURE 1 Flow diagram illustrating the comparison of the present and the existing methods.

$$\left(\lambda_m^2 M + \lambda_m C + K\right)^T \frac{\partial\tilde{V}_m}{\partial q} = -(2\lambda_m M + C)^T\tilde{V}_m\frac{\partial\chi_m}{\partial q} - \left(\lambda_m^2\frac{\partial M}{\partial q} + \lambda_m\frac{\partial C}{\partial q} + \frac{\partial K}{\partial q}\right)^T\tilde{V}_m \tag{41b}$$

$$\left(\lambda_i^2 M + \lambda_i C + K\right)\frac{\partial\tilde{\varphi}_i}{\partial q} = -\left(2\lambda_i M + C\right)\tilde{\varphi}_i\frac{\partial\lambda_i}{\partial q} - \left(\lambda_i^2\frac{\partial M}{\partial q} + \lambda_i\frac{\partial C}{\partial q} + \frac{\partial K}{\partial q}\right)\tilde{\varphi}_i \tag{42a}$$

$$\left(\lambda_i^2 M + \lambda_i C + K\right)^T\frac{\partial\tilde{\psi}_i}{\partial q} = -(2\lambda_i M + C)^T\tilde{\psi}_i\frac{\partial\lambda_i}{\partial q} - \left(\lambda_i^2\frac{\partial M}{\partial q} + \lambda_i\frac{\partial C}{\partial q} + \frac{\partial K}{\partial q}\right)^T\tilde{\psi}_i \tag{42b}$$

As stated earlier, These issues are well recognized and can be overcome by utilizing Nelson[16] technique which was widely known as the powerful technique for solving the nonsingular problem by many researchers (e.g., Mills-Curran,[17] Nelson,[16] Ojalvo,[18] Dailey[19]). And due to the normalization equations equal to one (constant) in Equation (18) for the

problem with the repeated eigenvalue and Equation (31) for the problem with the distinct eigenvalue, the authors suggest justifying Nelson[16] techniques by deleting the row and column of the denominator matrix and deleting the row of the numerator vector corresponding to the component with respect to the normalization in Equations (19) and (32). Therefore, numerical stability can be maintained and guaranteed. As a result, by utilizing Equations (41) or (42), the chain rule technique can be applied, and consequently, the eigenvector sensitivities can be easily computed. Moreover, this proposed method is simple and easy to implement and build the in-house codes in combination with the finite element method, which has been proven to be an efficient method for solving the elastic and plastic problems in structure and geomechanics.[40–45]

3 | NUMERICAL EXAMPLES

To illustrate the validity of the proposed method, five examples are raised and considered in this paper. For the first example, the eigensolution sensitivities of a damped rigid rotor on flexible supports, which are modeled using the springs and dashpots, are solved with the distinct eigenvalue. The second is contemplated a three-degrees of freedom rotordynamic model, which is an asymmetric damped system and consists of five springs, four damping, and three disks. This example is focused on the derivatives of eigenvalue and eigenvector with both distinct and repeated eigenvalues. Moreover, the eigensolution derivatives of the finite element rotordynamic system are also numerically computed and provided, as in example 3. Consequently, in order to validate the proposed method, the approximated results of the linear approximation of the perturbed system are calculated by Taylor series and compared with the actual results, where the expression of the approximated results[1,3] is written as

$$\tilde{\Theta}_{changed} = \Theta_{initial} + \frac{\partial \Theta}{\partial q}\Delta q \tag{43}$$

And the errors (Er) can be determined by

$$Er(\%) = \frac{\left|\tilde{\Theta}_{changed} - \Theta_{changed}\right|}{\Theta_{changed}} \times 100 \tag{44}$$

where, $\Theta_{initial}, \Theta_{changed}, \tilde{\Theta}_{changed}$ andΔq are the eigensolution's initial value, the eigensolution's actual value, the approximated value of the eigensolution, and the change in design parameter, respectively. All simulations are performed by the in-house codes written in the framework of Matlab R2017b on an Intel® Core™ i7-4770 CPU @3.4GHz processors and 32GB RAM.

3.1 | Example 1

This example presents the calculation of the sensitivity analysis of the eigensolution with the distinct eigenvalue of the asymmetric system for the rotordynamic model,[1,2,13] as shown in Figure 2, in which the mass, damping the stiffness matrices are provided below. In addition, by choosing the real parameter q as the mass of the rotor, one set $q_0 = 122.68$ and therefore,

$$M = \begin{bmatrix} m_0 & 0 & 0 & 0 \\ 0 & m_0 & 0 & 0 \\ 0 & 0 & 2.8625 & 0 \\ 0 & 0 & 0 & 2.8625 \end{bmatrix} \Rightarrow \frac{\partial M}{\partial q} = \begin{bmatrix} 1 & 0 & 0 & 0 \\ 0 & 1 & 0 & 0 \\ 0 & 0 & 0 & 0 \\ 0 & 0 & 0 & 0 \end{bmatrix}$$

$$K = 1e6 \times \begin{bmatrix} 2.1 & 0 & 0 & 0.025 \\ 0 & 3 & -0.05 & 0 \\ 0 & -0.05 & 0.1875 & 0 \\ 0.025 & 0 & 0 & 0.13125 \end{bmatrix} \Rightarrow \frac{\partial K}{\partial q} = 0$$

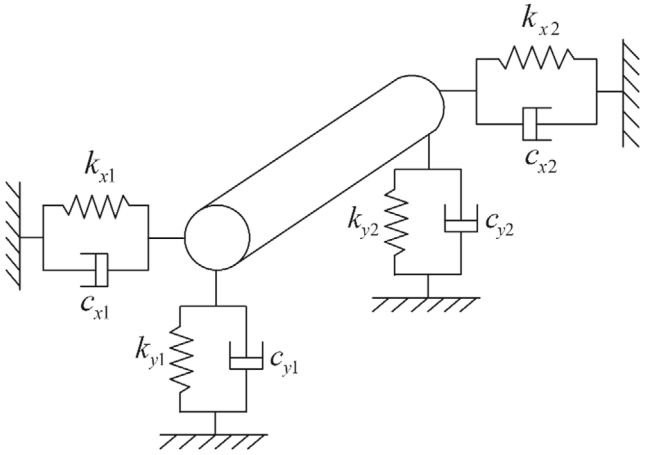

FIGURE 2 A damped rigid rotor on flexible supports.

TABLE 1 Comparison of the eigenvalues for the distinct eigenvalue problem of example 1.

Mode no	Eigenvalues $\lambda_{initial}$	Eigenvalues derivatives $\partial\lambda/\partial q$	Eigenvalues $\lambda_{changed}$	Eigenvalues $\tilde{\lambda}_{changed}$	Error (%)
1	$-8.225 + 130.172i$	$6.877e-2 - 0.522i$	$-8.156 + 129.653i$	$-8.156 + 129.650i$	0.0023
2	$-8.225 - 130.172i$	$6.877e-2 + 0.522i$	$-8.156 - 129.653i$	$-8.156 - 129.650i$	0.0023
3	$-10.405 + 153.514i$	$0.335 - 0.389i$	$-10.084 + 153.099i$	$-10.070 + 153.125i$	0.0192
4	$-10.405 - 153.514i$	$0.335 + 0.389i$	$-10.084 - 153.099i$	$-10.070 - 153.125i$	0.0192
5	$-11.652 + 159.217i$	$-0.271 - 0.252i$	$-11.909 + 158.994i$	$-11.923 + 158.965i$	0.0202
6	$-11.652 - 159.217i$	$-0.271 + 0.252i$	$-11.909 - 158.994i$	$-11.923 - 158.965i$	0.0202
7	$-29.689 + 347.527i$	$-1.685e-4 - 9.618e-4i$	$-29.689 + 347.526i$	$-29.689 + 347.526i$	0.0000
8	$-29.689 - 347.527i$	$-1.685e-4 + 9.618e-4i$	$-29.689 - 347.526i$	$-29.689 - 347.526i$	0.0000

$$C = 1e3 \times \begin{bmatrix} 2 & 0 & 0 & 0 \\ 0 & 2 & 0 & 0 \\ 0 & 0 & 0.125 & 0.53315 \\ 0 & 0 & -0.53315 & 0.125 \end{bmatrix} \Rightarrow \frac{\partial C}{\partial q} = 0$$

As a result, four pairs of the conjugate complex eigenvalues of the initial system are computed such as $-8.225 \pm 130.172i$, $-10.405 \pm 153.514i$, $-11.652 \pm 159.217i$, and $-29.689 \pm 347.527i$. When $m_0 = q = 122.68$, and Equation (4b) is employed to normalize the right and left eigenvectors, the eigenvalue derivatives can be computed as in Table 1. In addition, to validate the proposed method, we perturb m by $\Delta m = \Delta q = 1$. It is found that the calculated eigenvalue derivatives are in excellent agreement with those computed by the approximated method, in which the calculated maximum error is about 0.0202%, as seen in Table. 1.

Moreover, to validate the proposed method in calculating the sensitivity analysis of the eigenvectors, the computed result is only listed for those corresponding to the eigenvalue $\lambda_7 = -29.689 + 347.527i$. Unlike the eigenvalue derivative, the eigenvectors derivatives require another normalization condition (see Equation 31). Subsequently, the derivatives of the right and left eigenvectors can be computed by the proposed method and presented in Tables 2 and 3, respectively. Also, the verifications are carried out with the results computed by the approximated method. It is observed that reliable agreements are met between the two. More precisely, the maximum errors are respectively 0.5048% and 1.1621% provided at the second degree of freedom for right and left eigenvectors. Obviously, the computed eigensolutions and the eigensolution derivatives in Tables 1, 2, and 3 are all satisfied with Equations (2a), (2b), and (4b). Consequently, the normalizations of the computational procedures used in this note are consistent for the entire system.

TABLE 2 Comparison of the right eigenvectors for the distinct eigenvalue problem of example 1.

DOF	Eigenvector φ_7	Eigenvector derivatives $\partial\varphi_7/\partial q$	Eigenvector $\varphi_{changed}$	Eigenvector $\tilde{\varphi}_{changed}$	Error (%)
1	$-2.682e-5-1.971e-5i$	$1.248e-7+9.697e-8i$	$-2.658e-5-1.952e-5i$	$-2.670e-5-1.962e-5i$	0.4698
2	$-4.767e-5+6.817e-5i$	$2.488e-7-3.440e-7i$	$-4.717e-5+6.749e-5i$	$-4.742e-5+6.783e-5i$	0.5048
3	$0.0137-0.0143i$	$0.0000+0.0000i$	$0.0137+0.0143i$	$0.0137+0.0143i$	0.0004
4	$-0.0121-0.0120i$	$-2.920e-8-1.836e-8i$	$-0.0121-0.0120i$	$-0.0121-0.0120i$	0.0006

TABLE 3 Comparison of the left eigenvectors for the distinct eigenvalue problem of example 1.

DOF	Eigenvector φ_7	Eigenvector derivatives $\partial\varphi_7/\partial q$	Eigenvector $\varphi_{changed}$	Eigenvector $\tilde{\varphi}_{changed}$	Error (%)
1	$2.682e-5-1.971e-5i$	$1.022e-7+1.211e-7i$	$-2.658e-5-1.952e-5i$	$-2.693e-5-1.960e-5i$	1.0810
2	$-4.767e-5-6.817e-5i$	$3.341e-7-2.629e-7i$	$-4.717e-5+6.749e-5i$	$-4.733e-5+6.843e-5i$	1.1621
3	$0.0137+0.0143i$	$0.0000+0.0000i$	$0.0137+0.0143i$	$0.0137+0.0143i$	0.0004
4	$0.0121-0.0120i$	$-5.394e-8-4.515e-8i$	$-0.0121-0.0120i$	$-0.0121-0.0120i$	0.0008

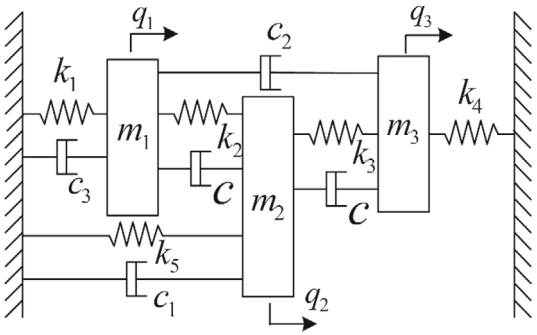

FIGURE 3 The three degrees of freedom rotor dynamic model.

Furthermore, for additional validation of the developed algorithm with the approximate method, two more design variables ($\Delta q = 1.2268$ (proportion of $\frac{1.2268}{122.68} = 1\%$) and 2.4536 (proportion of $\frac{2.4536}{122.68} = 2\%$)) are selected to compute the errors. Consequently, the derivatives of the right and left eigenvectors are determined and tabulated in Tables S1–S4 in the Supplemental Material (SM) for $\Delta q = 1.2268$ and 2.4536, respectively. It is found that the maximum error between the exact and approximate eigenvectors are respectively found to be 1.42% and 2.86% for $\Delta q = 1.2268$ and $\Delta q = 2.4536$. These computed errors reveal a consistent increase as the design variables increase, suggesting that the proposed method in this manuscript consistently generates acceptable errors. Hence, the accuracy and efficiency of the present method can be deemed satisfactory.

3.2 | Example 2

In contrast to the first example, the second example presents the computation of the eigenvalue and eigenvector derivatives with both the distinct and the repeated eigenvalues of a three degrees of freedom rotordynamic model.[1,3] The asymmetric damped model is illustrated in Figure 3, in which the mass, damping, and stiffness matrices are respectively provided by

$$M = \begin{bmatrix} m_1 + m_0 & 0 & 0 \\ 0 & m_2 + m_0 & 0 \\ 0 & 0 & m_3 + m_0 \end{bmatrix}$$

$$K = \begin{bmatrix} k_1 + k_2 & -k_2 & 0 \\ -k_2 & k_2 + k_3 + k_5 & -k_3 \\ 0 & -k_3 & k_3 + k_4 \end{bmatrix}$$

$$D = \begin{bmatrix} c_2 + c_3 + c_4 & -c_4 & -c_2 \\ -c_4 & c_1 + 2c_4 & -c_4 \\ -c_2 & -c_4 & c_2 + c_4 \end{bmatrix}$$

The gyroscopic matrix of the computed rotordynamic model is assumed by

$$G = \begin{bmatrix} 0 & -c_4 & -c_2 \\ c_4 & 0 & -c_4 \\ c_2 & c_4 & 0 \end{bmatrix}$$

Consequently, the system of the damping matrix becomes

$$C = D + G = \begin{bmatrix} c_2 + c_3 + c_4 & -2c_4 & -2c_2 \\ 0 & c_1 + 2c_4 & -2c_4 \\ 0 & 0 & c_2 + c_4 \end{bmatrix}$$

Let us assume $m_1 = m_2 = m_3 = 2.5$ kg, $k_1 = k_4 = k_5 = 2000$ N/m, $k_2 = k_3 = 0$ N/m, $c_1 = c_2 = c_3 = 10$ N $\cdot$ s/m and $c_4 = 0$ N $\cdot$ s/m. The mass m_0 is chosen to be the design parameter q, and the eigensolution derivatives are considered at $m_0 = 0$ kg. Therefore,

$$M = \begin{bmatrix} 2.5 & 0 & 0 \\ 0 & 2.5 & 0 \\ 0 & 0 & 2.5 \end{bmatrix} \Rightarrow \frac{\partial M}{\partial q} = \begin{bmatrix} 1 & 0 & 0 \\ 0 & 1 & 0 \\ 0 & 0 & 1 \end{bmatrix}$$

$$K = \begin{bmatrix} 2000 & 0 & 0 \\ 0 & 2000 & 0 \\ 0 & 0 & 2000 \end{bmatrix} \Rightarrow \frac{\partial K}{\partial q} = \begin{bmatrix} 0 & 0 & 0 \\ 0 & 0 & 0 \\ 0 & 0 & 0 \end{bmatrix}$$

$$C = \begin{bmatrix} 20 & 0 & -20 \\ 0 & 10 & 0 \\ 0 & 0 & 10 \end{bmatrix} \Rightarrow \frac{\partial C}{\partial q} = \begin{bmatrix} 0 & 0 & 0 \\ 0 & 0 & 0 \\ 0 & 0 & 0 \end{bmatrix}$$

The computations are performed by transforming the quadratic eigenproblem equations into the state-space equation (see Equation 3). As a result, the problem is solved with two distinct eigenvalues: $-4 + 28i$ and $-4 - 28i$, and two-repeated eigenvalues: $-2 + 28.2135i$ and $-2 - 28.2135i$.

- For distinct eigenvalue

In this case, to illustrate the procedure of the proposed methodology, the eigenvalue $(-10 + 28i)$ is employed. Consequently, the computed derivative of the eigenvalue using Equation (30b) is $1.6 - 5.4857i$. Using Equations (31) and (33), the right and left eigenvectors calculated are

$$\eta = \begin{bmatrix} 0.0598 - 0.0598i \\ 0 \\ 0 \\ 1.4343 + 1.9124i \\ 0 \\ 0 \end{bmatrix}, \quad \xi = \begin{bmatrix} 0.0598 + 0.0598i \\ 0 \\ -0.195 - 0.1195i \\ 1.4343 - 1.9124i \\ 0 \\ -2.8685 + 3.8247i \end{bmatrix}$$

Finally, the eigenvector sensitivities can be computed by employing Equations (40a) and (40b).

$$\frac{\partial \eta}{\partial q} = \begin{bmatrix} 0.0068 - 0.0051i \\ 0 \\ 0 \\ 0 \\ 0 \\ 0 \end{bmatrix}, \frac{\partial \xi}{\partial q} = \begin{bmatrix} -0.0068 + 0.0051i \\ 0 \\ 0.0137 - 0.0102i \\ 0 \\ 0 \\ 0 \end{bmatrix}$$

Similar to Example 1, to demonstrate the validation of the proposed method, we perturb m by $\Delta m = \Delta q = 0.025$. Table 4 presents the comparisons of the magnitudes of the right eigenvectors computed by the present and the approximated methods. Similarly, Table 5 is for the left eigenvectors. It is observed that the eigensolutions calculated in Tables 4 and 5 are all obeyed the normalization Equations (3a), (3b), and (4a). Therefore, the normalization conditions are consistent. Moreover, it is found that reasonable agreements are obtained, and the maximum error is 0.7575% given by the right and the left eigenvectors. Therefore, from the engineering perspective, it may conclude that the proposed method may provide good results for solving the distinct eigenvalue problem.

TABLE 4 Comparison of the right eigenvectors for the distinct eigenvalue of example 2.

DOF	Eigenvector η_1	Eigenvector derivatives $\partial\eta_1/\partial q$	Eigenvector $\eta_{changed}$	Eigenvector $\tilde{\eta}_{changed}$	Error (%)
1	$0.0598 - 0.0598i$	$0.0068 - 0.0051i$	$0.0596 - 0.0596i$	$0.0599 - 0.0599i$	0.5060
2	0	0	0	0	0
3	0	0	0	0	0
4	$1.4343 + 1.9124i$	0	$1.4249 + 1.8970i$	$1.4343 + 1.9124i$	0.7575
5	0	0	0	0	0
6	0	0	0	0	0

TABLE 5 Comparison of the left eigenvectors for the distinct eigenvalue of example 2.

DOF	Eigenvector ξ_1	Eigenvector derivatives $\partial\xi_1/\partial q$	Eigenvector $\xi_{changed}$	Eigenvector $\tilde{\xi}_{changed}$	Error (%)
1	$0.0598 + 0.0598i$	$-0.0068 + 0.0051i$	$0.0596 + 0.0596i$	$0.0596 + 0.0596i$	0.3324
2	0	0	0	0	0
3	$-0.1195 - 0.1195i$	$0.0137 - 0.0102i$	$-0.1192 - 0.1192i$	$-0.1192 - 0.1198i$	0.3324
4	$1.4343 - 1.9124i$	0	$1.4249 - 1.8970i$	$1.4343 - 1.9124i$	0.7575
5	0	0	0	0	0
6	$-2.8685 + 3.8247i$	0	$-2.8498 + 3.7941i$	$-2.8685 + 3.8247i$	0.7575

- For repeated eigenvalue

The two-repeated eigenvalue $(-2+28.2135i)$ is contemplated in this case. By using solving the eigenproblem in Equation (14), the derivative of the eigenvalues is

$$\frac{\partial \chi_m}{\partial q} = \frac{\partial \lambda_l}{\partial q} I_m = \begin{bmatrix} 0.8-5.6143i & 0 \\ 0 & 0.8-5.6143i \end{bmatrix}$$

After normalization, the magnitudes of the σ and τ are

$$\sigma = \begin{bmatrix} 0 & 1 \\ 1 & 0 \end{bmatrix}, \tau = \begin{bmatrix} 0 & 1 \\ 1 & 0 \end{bmatrix}$$

The right and left eigenvectors normalized by Equation (18) are

$$\tilde{U}ss_m = \begin{bmatrix} 0 & -0.0050-0.0705i \\ -0.0025-0.0353i & 0 \\ 0 & -0.0025-0.0353i \\ 0 & 2.0000-0.0000i \\ 1.0000+0.0000i & 0 \\ 0 & 1.0000+0.0000i \end{bmatrix}$$

$$\tilde{V}ss_m = \begin{bmatrix} 0 & 0 \\ -0.0025+0.0353i & 0 \\ 0 & -0.0025+0.0353i \\ 0 & 0 \\ 1.0000+0.0000i & 0 \\ 0 & 1.0000+0.0000i \end{bmatrix}$$

Consequently, the right and left eigenvectors calculated by Equation (21b) are

$$uss_m = \begin{bmatrix} 0 & 0.1191-0.1191i \\ 0.0595-0.0595i & 0 \\ 0 & 0.0595-0.0595i \\ 0 & 3.1212+3.5975i \\ 1.5606+1.7988i & 0 \\ 0 & 1.5606+1.7988i \end{bmatrix}$$

$$vss_m = \begin{bmatrix} 0 & 0 \\ 0.0595+0.0595i & 0 \\ 0 & 0.0595+0.0595i \\ 0 & 0 \\ 1.5606-1.7988i & 0 \\ 0 & 1.5606-1.7988i \end{bmatrix}$$

Finally, employing Equations (40a) and (40b), the derivatives of the eigenvectors can be computed:

$$\frac{\partial uss_m}{\partial q} = \begin{bmatrix} 0 & -0.0128 - 0.0111i \\ -0.0064 - 0.0055i & 0 \\ 0 & -0.0064 - 0.0055i \\ 0 & 0 \\ 0 & 0 \\ 0 & 0 \end{bmatrix}$$

$$\frac{\partial vss_m}{\partial q} = \begin{bmatrix} 0 & 0 \\ 0.0154 + 0.0196i & 0 \\ 0 & 0.0154 + 0.0196i \\ 0 & 0 \\ 0 & 0 \\ 0 & 0 \end{bmatrix}$$

Tables 6 and 7 illustrate the comparisons of the values of the eigenvectors computed by the present method and the approximated method for the right and the left eigenvectors, respectively. Likewise, the eigensolutions calculated in Tables 6 and 7 are conformed with the normalization Equations (3a), (3b), and (4a); consequently, the normalization conditions are consistent. As a result, close agreements are found, and the maximum errors are respectively 0.7511% and 0.9911% produced by the right and the left eigenvectors. Thus, from the engineering point of view, it can infer that the proposed method can produce good results by solving the repeated eigenvalue problem.

Additionally, to further validate the developed algorithm in comparison with the approximate method, two additional design variables ($\Delta q = 0.050$ (proportion of $\frac{0.050}{2.5} = 2\%$) and 0.075 (proportion of $\frac{0.075}{2.5} = 3\%$)) are chosen to calculate the errors. As a result, the derivatives of the right and left eigenvectors are determined and presented in Tables S5–S8 in the SM for $\Delta q = 0.050$ and 0.075, respectively. The maximum errors between the exact and approximate eigenvectors are observed to be 1.98% and 2.98% for $\Delta q = 0.050$ and $\Delta q = 0.075$, respectively. These computed errors consistently increase as the design variables become larger, indicating that the proposed method in this manuscript consistently yields errors within acceptable ranges. Therefore, the accuracy and efficiency of the present method can be considered satisfactory.

TABLE 6 Comparison of the right eigenvectors for the repeated eigenvalue problem of example 2.

DOF	Eigenvector uss_m	Eigenvector derivatives $\partial uss_m/\partial q$	Eigenvector $uss_{changed}$	Eigenvector $\tilde{uss}_{changed}$	Error (%)
1	0	0	0	0	0
2	$0.0595 - 0.0595i$	$-0.0064 - 0.0055i$	$0.0594 - 0.0594i$	$0.0594 - 0.0597i$	0.3419
3	0	0	0	0	0
4	0	0	0	0	0
5	$1.5606 + 1.7988i$	0	$1.5496 + 1.7848i$	$1.5606 + 1.7988i$	0.7511
6	0	0	0	0	0
1	$0.1191 - 0.1191i$	$-0.0128 - 0.0111$	$0.1188 - 0.1188i$	$0.1188 - 0.1193i$	0.3419
2	0	0	0	0	0
3	$0.0595 - 0.0595i$	$-0.0064 - 0.0055i$	$0.0594 - 0.0594i$	$0.0594 - 0.0597i$	0.3419
4	$3.1212 + 3.5976i$	0	$3.0992 + 3.5696i$	$3.1212 + 3.5975i$	0.7511
5	0	0	0	0	0
6	$1.5606 + 1.7988i$	0	$1.5496 + 1.7848i$	$1.5606 + 1.7988i$	0.7511

TABLE 7 Comparison of the left eigenvectors for the repeated eigenvalue problem of example 2.

DOF	Eigenvector vss_m	Eigenvector derivatives $\partial vss_m/\partial q$	Eigenvector $vss_{changed}$	Eigenvector $\tilde{vss}_{changed}$	Error (%)
1	0	0	0	0	0
2	$0.0595 + 0.0595i$	$0.0194 + 0.0196i$	$0.0594 + 0.0594i$	$0.0599 + 0.0600i$	0.9911
3	0	0	0	0	0
4	0	0	0	0	0
5	$1.5606 - 1.7988i$	0	$1.5496 - 1.7848i$	$1.5606 - 1.7988i$	0.7511
6	0	0	0	0	0
1	0	0	0	0	0
2	0	0	0	0	0
3	$0.0595 + 0.0595i$	$0.0194 + 0.0196i$	$0.0594 - 0.0594i$	$0.0599 - 0.0600i$	0.9911
4	0	0	0	0	0
5	0	0	0	0	0
6	$1.5606 - 1.7988i$	0	$1.5496 + 1.7848i$	$1.5606 - 1.7988i$	0.7511

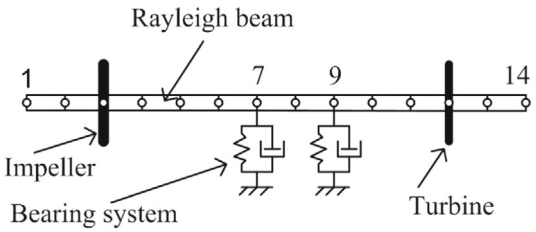

FIGURE 4 The finite element rotating shaft model of the turbocharger.

TABLE 8 The geometrical parameters of the rotating shaft.

Element number	1	2	3	4	5	6	7	8	9	10	11	12	13
Length (mm)	3.4	4.5	15.2	6	7.1	9.5	12.65	16.15	3	11.2	6.6	9.6	3.3
Diameter (mm)	4.1	4.1	4.1	4.1	4.1	6	6	6	6	9.9	14.2	11	8

3.3 | Example 3

The finite element rotating shaft model of the turbocharger,[46] as illustrated in Figure 4, is used in this example. This rotor model is an asymmetric damped system. The geometrical parameters of the model are tabulated in Table 8. The rotor shaft is discretized into 13 Rayleigh beam elements which have 14 nodes in total and four degrees of freedom at each node, and consequently, the number of DOFs in total is 64. The parameters of the rigid disks as an impeller are provided at node 3 with the mass, the diametral inertia (I_d), and polar inertia (I_p) by $m_d = 1.3328e^{-2}$ kg, $I_d = 1.274e^{-6}$ kgm^2 and $I_p = 2.156e^{-6}$ kgm^2, respectively. In addition, at node 12, a turbine (rigid disk) is also installed with $m_d = 4.3414e^{-2}$ kg, $I_d = 3.136e^{-6}$ kgm^2 and $I_p = 5.88e^{-6}$ kgm^2. Also, the same spring support coefficients of the bearing are given at nodes 7 and 9 with the stiffness $k_{xx} = k_{yy} = 10^6$ N/m and damping $c_{xx} = c_{yy} = 3$ Ns/m. The material properties of the rotor model are Young's modulus of $2.1e^{11}$ N/m^2 and density of 7800 kg/m^3. It is worth noting that the gyroscopic effects are included in this finite element rotordynamic system, and the formulations of the Rayleigh beam and the rigid disk are available in Appendix A, for the fixed reference system (for detail, you may refer to References 47, 48).

Figure 5 presents the Campbell diagram for the first 10 modes computed in this example. To establish this diagram, the rotational speeds are applied from 0 to 5000 (Hz) with an increment of 500 (Hz). From the intersection of the forward whirling (FW) mode lines with the 1P line in this diagram for the fixed reference system, the values of the critical

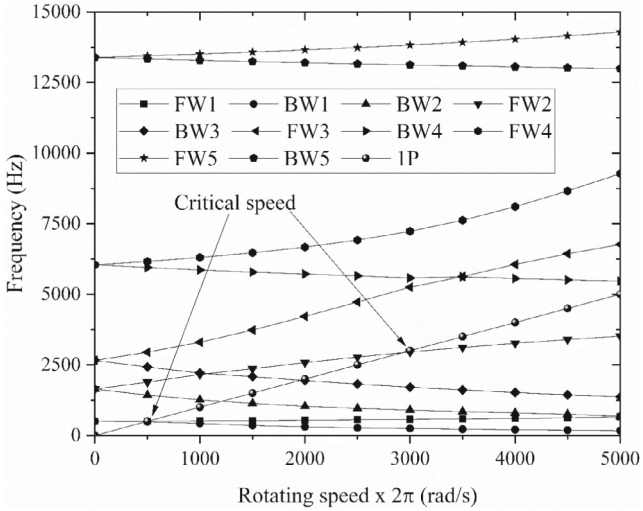

FIGURE 5 Campbell diagram of the finite element turbocharger.

TABLE 9 Computation of the eigenvalues and their derivatives.

Number of modes	Eigenvalues λ	Eigenvalues derivatives $\partial\lambda/\partial q$
1	$-3.2577e-1-1.7086e+3i$	$-5.2604e+4+4.4617e+7i$
2	$-3.2577e-1+1.7086e+3i$	$-5.2604e+4-4.4617e+7i$
3	$1.7829e+3-6.3080e+2i$	$-1.4825e+8-4.6234e+8i$
4	$1.7829e+3+6.3080e+2i$	$-1.4825e+8+4.6234e+8i$
⋮	⋮	⋮
57	$-2.9933e+1-1.0075e+6i$	$2.3750e+6+6.7780e+8i$
58	$-2.9933e+1+1.0075e+6i$	$2.3750e+6-6.7780e+8i$
59	$-3.0201e+1-1.0078e+6i$	$-2.2688e+6+7.0625e+8i$
60	$-3.0201e+1+1.0078e+6i$	$-2.2688e+6-7.0625e+8i$

speeds (Ω_{Cr}) of the first and second FW modes are respectively found at about 500 Hz and 3000 Hz (or 30,000 rpm and 180,000 rpm). And it is found that these computed results are in good agreement with the existing results produced by Straub.[46]

To illustrate the computation of the eigensolution derivatives, the design parameters q to be the shaft diameter and shaft length of each element are chosen, and the rotational speed value is selected at 2500 (Hz) (the central value of rotating speed). It is worth noting that the modal superposition-based model order reduction[40] is also applied with a total basis of $n = 30$. Consequently, the dimension of the reduced DOF in the state-space equation is $2n = 60$. Subsequently, the eigenvalues and their derivatives are computed by using Equation (30b) and tabulated in Table 9. In addition, Tables 10 and 11 provide the right and left eigenvectors and their derivatives computed by employing Equations (40a) and (40b) for the first eigenvalue (i.e., $\lambda_1 = -3.2577e-1-1.7086e+3i$), respectively. Moreover, the right and left eigenvectors and their derivatives for $\lambda_{60} = -3.0201e+1+1.0078e+6i$ can also be calculated and respectively tabulated in Tables 12 and 13. Similarly, it is observed that the calculated results in Tables 9–13 are obeyed the normalization Equations (3a), (3b), and (4a); and consequently, the normalization conditions are consistent. Moreover, numerical stability can also be achieved.

3.4 | Example 4

A rotating simply supported shaft, which has a slenderness ratio of 0.1[48] as seen in Figure 6, is utilized to conduct the sensitivity analysis in 3D finite element in the co-rotating reference system. Thus, the Coriolis effect is taken into

TABLE 10 Computation of the right eigenvectors and their derivatives for the eigenvalue λ_1.

Reduced DOF	Right eigenvector η	Right eigenvalues derivatives $\partial\eta/\partial q$
1	$0.0871 - 0.6859i$	$-2.3364e+4 - 5.4131e+4i$
2	$-0.1496 - 0.2971i$	$3.9338e+4 - 3.0690e+4i$
3	$0.0451 + 0.3549i$	$-1.2428e+4 + 4.4840e+3i$
4	$-1.5328 + 0.0013i$	$-7.1192e+4 + 6.3546e+1i$
⋮	⋮	⋮
57	$-0.0022 + 0.0418i$	$1.3571e+1 - 1.2286e+3i$
58	$0.0117 + 0.0001i$	$2.0116e+3 + 4.2791e+0i$
59	$-0.0006 - 0.0134i$	$1.5680e+0 - 2.3480e+3i$
60	$-0.0033 + 0.0006i$	$3.8488e+3 - 3.5513e+0i$

TABLE 11 Computation of the left eigenvectors and their derivatives for the eigenvalue λ_1.

Reduced DOF	Left eigenvector ξ	Left eigenvalues derivatives $\partial\xi/\partial q$
1	$0.0766 - 0.1861i$	$6.1686e+10 + 2.3290e+11i$
2	$-0.1320 - 0.1021i$	$-1.0337e+11 + 1.0874e+11i$
3	$0.0416 + 0.0223i$	$3.0865e+10 - 1.0294e+11i$
4	$-0.0626 + 0.0003i$	$-2.2039e+11 + 1.6014e+9i$
⋮	⋮	⋮
57	$0.000 + 0.000i$	$-1.0739e+1 - 2.8748e+3i$
58	$0.000 + 0.000i$	$2.6309e+3 + 1.2355e+1i$
59	$0.000 + 0.000i$	$4.5178e+0 - 2.2497e+3i$
60	$0.000 + 0.000i$	$3.4253e+3 - 5.5766e+0i$

TABLE 12 Computation of the right eigenvectors and their derivatives for the eigenvalue λ_{60}.

Reduced DOF	Right eigenvector η	Right eigenvalues derivatives $\partial\eta/\partial q$
1	$0.000 + 0.000i$	$-2.6951e-5 + 4.2669e-4i$
2	$0.000 + 0.000i$	$-1.7491e-5 - 6.8841e-4i$
3	$0.000 + 0.000i$	$3.7107e-5 + 2.1854e-4i$
4	$0.000 + 0.000i$	$9.8676e-6 + 7.7419e-4i$
⋮	⋮	⋮
57	$-0.0044 - 0.0001i$	$-4.5762e+3 + 4.8731e+1i$
58	$0.0002 + 0.0038i$	$1.5387e+2 - 7.6244e+2i$
59	$0.5013 + 0.0001i$	$0.000 + 0.000i$
60	$0.0044 + 0.5236i$	$6.0543e+3 + 4.7666e+5i$

TABLE 13 Computation of the left eigenvectors and their derivatives for the eigenvalue λ_{60}.

Reduced DOF	Left eigenvector ξ	Left eigenvalues derivatives $\partial\xi/\partial q$
1	$4.3754 + 0.9066i$	$-9.9582e+6 + 3.3756e+4i$
2	$2.7815 - 1.6520i$	$-6.3670e+6 + 1.5808e+5i$
3	$0.6390 + 0.4974i$	$-1.5292e+6 - 1.7821e+4i$
4	$-0.0185 - 5.0641i$	$2.0910e+4 + 6.0758e+5i$
⋮	⋮	⋮
57	$0.000 + 0.000i$	$-6.6136e+3 + 5.2235e+1i$
58	$0.000 + 0.000i$	$3.4334e+2 - 2.5161e+2i$
59	$0.5013 - 0.0001i$	$0.000 + 0.000i$
60	$0.0039 + 0.4750i$	$-7.5809e+3 - 1.0259e+6i$

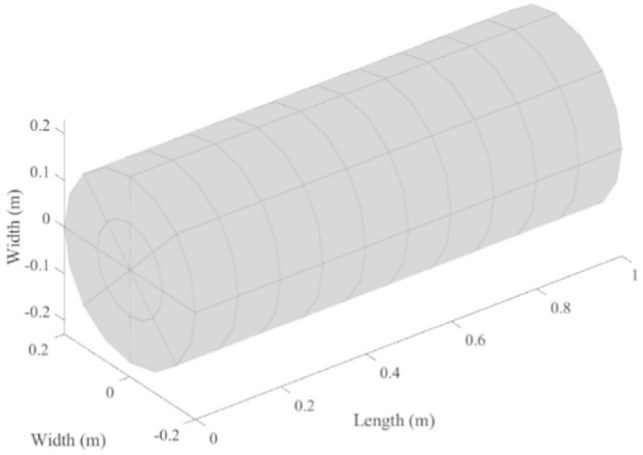

FIGURE 6 A rotating simply supported shaft in 3D finite element analysis.

computation.[40] The properties of the structure are Young's modulus (E_{shaft}) of $2e^{11}$ N/m^2, the density (ρ_{shaft}) of 7800 kg/m^3, Poisson's ratio of 0.3, the length of the shaft (l_{shaft}) of 1 m, and the radius of the shaft (R_{shaft}) of 0.2 m; consequently, the slenderness ratio is 0.1. This structure, which is an asymmetric system, is meshed with 709 nodes and 160 elements (80 15-node pentahedron elements and 80 20-node hexahedron elements), and 2127 degrees of freedom (DOFs). To perform the eigensensitivity analysis as well as verification of the responses of the model, the rotating speed is applied from 0 to 1000 Hz (0 to 60,000 rpm) with an increment of 200 Hz (12,000 rpm). In addition, the general equation of motion of the rotating structure in the co-rotating reference system in the three-dimensional finite element used in this example is given in Appendix B and the detail is found in References 40,49. It is also assumed that the simply supported boundary condition is applied at both ends of the rotating shaft.

Figure 7 illustrates the Campell diagram of the rotating simply supported shaft and it is found that critical speeds for the first and second forward whirling modes are respectively $\Omega_{Cr} = 749$ and 2358 Hz, and $\Omega_{Cr} = 666$ and 1950 Hz are for the first and second backward whirling modes, respectively. Consequently, by taking the present solution as the reference, the relative errors of the non-dimensional critical speed are -1.22%, and -5.32% for first and second forward whirling modes, 0.29% and 2.6% for first and second backward whirling modes as compared to those computed by Nelson[48] by using Timoshenko beam theory, in which the non-dimensional critical speed is expressed by $\left[\rho_{shaft} l_{shaft}^2 \Omega_{Cr}^2 / \left(E_{shaft} \times \left(R_{shaft}/2l_{shaft}\right)^2\right)\right]^{1/4}$.

In this example, to perform the eigensensitivity analysis, the density (ρ_{shaft}) of the rotating shaft is selected to be a design parameter q, while the speed of the rotation is taken at 400 (Hz) (24,000 rpm). Moreover, the modal superposition-based model order reduction, which is found to be an efficient technique to reduce the computational time for solving the rotordynamic system,[40] is also implemented with $n = 70$ in this example. Thus, the dimension of the system

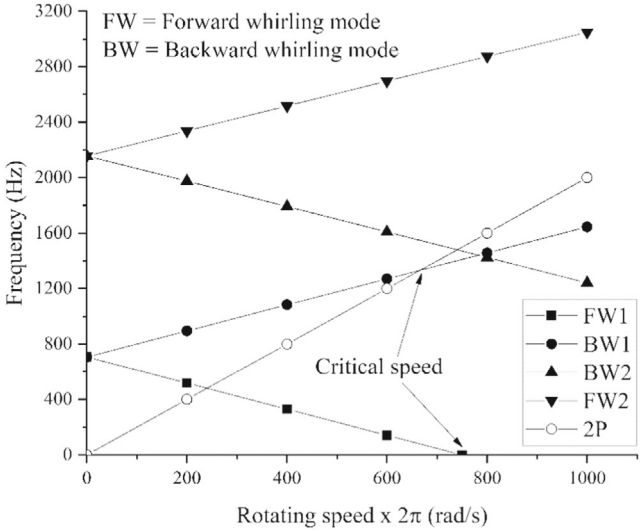

FIGURE 7 Campbell diagram of the rotating shaft.

TABLE 14 Computation of the eigenvalues and their derivatives.

Number of modes	Eigenvalues λ	Eigenvalues derivatives $\partial\lambda/\partial q$
1	$1.3379e-7-2.0474e+3i$	$-0.0000+0.2917i$
2	$1.0051e-5+2.0474e+3i$	$-0.0000-0.2917i$
3	$-2.3202e-9-3.7912e+3i$	$-0.0000+0.1403i$
4	$2.8110e-8+3.7912e+3i$	$0.0000-0.1403i$
⋮	⋮	⋮
137	$-9.5002e-11-6.5152e+4i$	$-0.0000+4.1884i$
138	$-8.6836e-11+6.5152e+4i$	$-0.0000-4.1884i$
139	$1.5565e-10-6.5681e+4i$	$0.0000+4.2076i$
140	$-7.3933e-11+6.5681e+4i$	$0.0000-4.2076i$

is reduced to $2n = 140$. As a result, by employing Equation (30b), the magnitudes of the eigenvalues and the eigenvalue derivatives can be computed as presented in Table 14. Furthermore, with the use of Equations (40a) and (40b), the right and left eigenvectors and their derivatives for the first eigenvalue (i.e., $\lambda_1 = 1.3379e-7-2.0474e+3i$) can be determined and provided in Tables 15 and 16, respectively. Likewise, for $\lambda_{140} = -7.3933e-11+6.5681e+4i$, the right and left eigenvectors and their derivatives might also be calculated as given in Tables 17 and 18, respectively. Similar to the previous examples, from the computed solutions in Tables 14–18, it is found that Equations (3a), (3b), and (4a) are conformed. Therefore, the normalization conditions are consistent and the numerical stability of the system is successfully achieved.

3.5 | Example 5

Another 3D finite element model of a shaft-disc-blade (SDB) assembly system, as illustrated in Figure 8, is also used to calculate the eigensolution derivatives. The geometrical properties of this structure are given in Table 19 and the structure, which is an asymmetric system, is generated with 45,685 nodes, 9504 elements (2160 15-node pentahedron elements and 7344 20-node hexahedron elements), and 137,055 DOFs. The material properties are Young's modulus (E_{SDB}) of 207.8 GPa, the density (ρ_{SDB}) of 7806 kg/m^3, and Poisson's ratio of 0.3. To carry out the analysis of the eigensolution derivatives, the rotating speed is applied from 0 to 1000 Hz (0 to 60,000 rpm) with an increment of 100 Hz (6000 rpm). It is noted that the general equation of motion of the rotating structure in the co-rotating reference system in the three-dimensional finite

TABLE 15 Computation of the right eigenvectors and their derivatives for the eigenvalue λ_1.

Reduced DOF	Right eigenvector η	Right eigenvalues derivatives $\partial\eta/\partial q$
1	$0.0000 + 0.0000i$	$-4.5345e-13 + 7.2893e-14i$
2	$-0.0568 + 0.5196i$	$4.6918e-13 - 1.6751e-12i$
3	$0.5227 + 0.0000i$	$0.0000 + 0.0000i$
4	$0.0000 + 0.0000i$	$-1.4232e-14 - 2.4548e-14i$
⋮	⋮	⋮
137	$0.0000 + 0.0000i$	$+3.5124e-18i$
138	$0.0000 + 0.0000i$	$+9.5521e-18i$
139	$0.0000 + 0.0000i$	$-1.7613e-18i$
140	$0.0000 + 0.0000i$	$4.8350e-15 - 1.2314e-14i$

TABLE 16 Computation of the left eigenvectors and their derivatives for the eigenvalue λ_1.

Reduced DOF	Left eigenvector ξ	Left eigenvalues derivatives $\partial\xi/\partial q$
1	$0.0000 + 0.0000i$	$-3.0724e-6 + 4.6894e-7i$
2	$-0.0568 + 0.5196i$	$1.0508e-5 - 2.9168e+2i$
3	$0.5227 + 0.0000i$	$0.0000 + 0.0000i$
4	$0.0000 + 0.0000i$	$-5.0255e-9 + 1.2556e-8i$
⋮	⋮	⋮
137	$0.000 + 0.000i$	$+1.5478e-17i$
138	$0.000 + 0.000i$	$+6.2927e-18i$
139	$0.000 + 0.000i$	$-1.6761e-17i$
140	$0.000 + 0.000i$	$-8.4444e-14 - 1.4715e-13i$

TABLE 17 Computation of the right eigenvectors and their derivatives for the eigenvalue λ_{140}.

Reduced DOF	Right eigenvector η	Right eigenvalues derivatives $\partial\eta/\partial q$
1	$0.000 + 0.000i$	$-3.1771e-22i$
2	$0.000 + 0.000i$	$+1.1100e-26i$
3	$0.000 + 0.000i$	$-2.7812e-26i$
4	$0.000 + 0.000i$	$-2.5588e-19i$
⋮	⋮	⋮
137	$0.0000 + 0.0000i$	$+2.5751e-18i$
138	$0.0482 + 0.4273i$	$-9.2229e-18i$
139	$0.4300 + 0.0001i$	$0.000 + 0.000i$
140	$0.0000 + 0.0000i$	$4.6097e-13 + 2.7355e-13i$

TABLE 18 Computation of the left eigenvectors and their derivatives for the eigenvalue λ_{140}.

Reduced DOF	Left eigenvector ξ	Left eigenvalues derivatives $\partial\xi/\partial q$
1	$0.000 + 0.000i$	$-3.3585e-13 + 5.6555e-13i$
2	$0.000 + 0.000i$	$2.3790e-15 - 3.4879e-19i$
3	$0.000 + 0.000i$	$1.0011e-15 - 1.1145e-18i$
4	$0.000 + 0.000i$	$3.4363e-11 + 2.0390e-11i$
⋮	⋮	⋮
137	$0.0000 + 0.0000i$	$1.0772e-16 + 9.6699e-17i$
138	$0.0482 + 0.4273i$	$2.0958e-16 - 2.1680e-4i$
139	$0.4300 + 0.0001i$	$0.000 + 0.000i$
140	$0.0000 + 0.0000i$	$-3.8815e-13 - 2.2958e-13i$

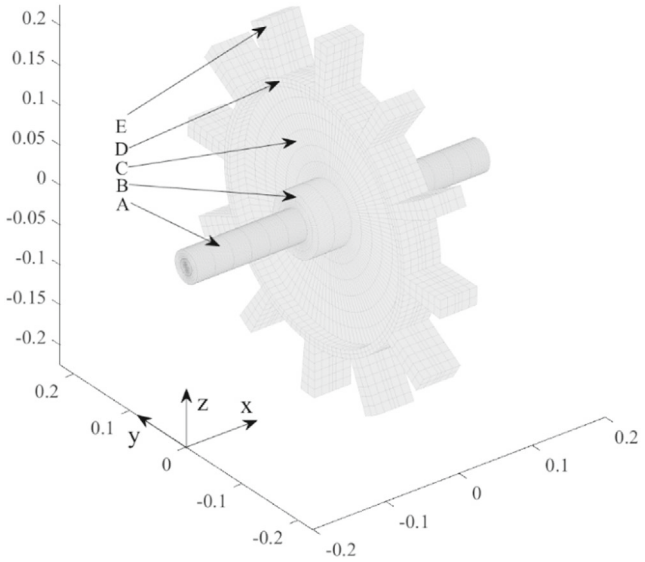

FIGURE 8 A shaft-disc-blade assembly model in 3D finite element.

element is used in this example as seen in Appendix B and the detail is referred to References 40,49. In addition, it is assumed that the simply supported boundary condition is applied at both ends of the structure.

Due to the large system, the model order reduction based on the modal superposition technique with the basis of $n = 80$ is used. Thus, the dimension of the system in this example is reduced to $2n = 160$. Consequently, the Campbell diagram of the shaft-disc-blade system can be established as seen in Figure 9. It is observed that the critical speeds for BW1, BW2, BW3, BW4, BW5, and BW6 modes (BW = backward whirling) are respectively found at 116, 220, 243, 500, 700, and 825 (Hz). Moreover, the critical speed for FW2 (FW = forward whirling) mode is found at 213 (Hz) or 12,780 (rpm). It is worth stating that the magnitudes of these critical speeds are computed and found to be agreed well with those computed by Phuor and Yoon[40] by employing the modal superposition-based model order reduction with a $n = 60$ basis.

Similar to Example 4, the density (ρ_{SDB}) of the rotating shaft-disc-blade (SDB) system is chosen to be a design parameter q to conduct the derivative of the eigensolutions and the speed of the rotation is considered at 600 (Hz) (36,000 rpm) in this example. Also, it should be noted that the fast assembly technique of the element matrices[50] in the finite element method combined with the parallel for-loop in Matlab is implemented. Accordingly, with the employment of Equation (30b), the eigenvalues and their derivatives of the system might be determined and tabulated in Table 20. Additionally, similar to the previous examples, for $\lambda_1 = 9.2688e-8-1.7924e+3i$, the right and left eigenvectors and their derivatives may be calculated and given in Tables 21 and 22, respectively. In the same way, for $\lambda_{160} = 6.1889e-9+4.9606e+4i$, the right and left eigenvectors and their derivatives can also be computed as provided in Tables 23 and 24, respectively. Similar

TABLE 19 Geometrical properties of the shaft, disc, and blade.

Structures (see Figure 8)	Dimension (m)		
	Length	Inner radius	Outer radius
A	0.4	0	0.02
B	0.1	0.02	0.04
C	0.01	0.04	0.15
D	0.05	0.15	0.16
E	12@0.05 with the revolution of 6°	0.16	0.225

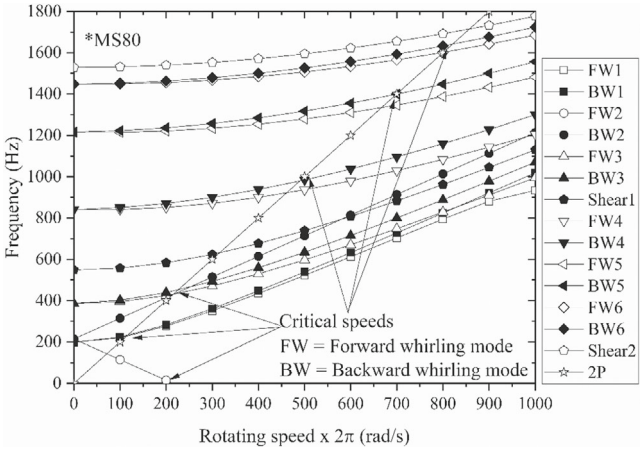

FIGURE 9 Campbell diagram of a shaft-disc-blade system in 3D finite element.

TABLE 20 Computation of the eigenvalues and their derivatives.

Number of modes	Eigenvalues λ	Eigenvalues derivatives $\partial\lambda/\partial q$
1	$9.2688e-8-1.7924e+3i$	$0.0000-0.0863i$
2	$-6.9545e-10+1.7924e+3i$	$0.0000+0.0863i$
3	$-2.7295e-7-3.2813e+3i$	$-0.0000+0.0307i$
4	$-1.5916e-8+3.2813e+3i$	$0.0000-0.0307i$
⋮	⋮	⋮
157	$-4.3042e-8-4.9399e+4i$	$0.0000+3.1223i$
158	$-5.0634e-8+4.9399e+4i$	$-0.0000-3.1223i$
159	$5.5881e-8-4.9606e+4i$	$0.0000+3.0986i$
160	$6.1889e-9+4.9606e+4i$	$0.0000-3.0986i$

to the aforementioned examples, from Tables 20 to 24, it is observed that Equations (3a), (3b), and (4a) are conformed; consequently, numerical stability is well obtained with consistent normalization conditions.

3.6 | Discussion on accuracy

Based on examples 1–2, it can be observed that the computed results obtained from the proposed method by not employing the second-order derivatives of the eigenequations exhibit errors of approximately 1% when compared to the results generated by the approximate method for the proportion of the design variable magnitude of about 1%. Consequently,

TABLE 21 Computation of the right eigenvectors and their derivatives for the eigenvalue λ_1.

Reduced DOF	Right eigenvector η	Right eigenvalues derivatives $\partial\eta/\partial q$
1	$0.0000 + 0.0000i$	$4.9462e-10 - 1.2963e-10i$
2	$0.0000 + 0.0000i$	$-7.5451e-9 - 5.5791e-9i$
3	$0.0007 + 0.0013i$	$-1.3596e-8 - 2.0972e-9i$
4	$-27.8334 + 39.7377i$	$-2.1221e-12 + 2.0205e-10i$
⋮	⋮	⋮
157	$-1.1554 - 0.7952i$	$-3.4547e-5 - 3.9593e-5i$
158	$-0.2660 - 1.3663i$	$-1.2219e-6 - 6.1989e-5i$
159	$0.0409 + 0.0158i$	$4.3813e-7 - 2.3050e-7i$
160	$0.0060 + 0.0006i$	$5.4979e-6 - 3.9324e-6i$

TABLE 22 Computation of the left eigenvectors and their derivatives for the eigenvalue λ_1.

Reduced DOF	Left eigenvector ξ	Left eigenvalues derivatives $\partial\xi/\partial q$
1	$1.9650e-6 - 6.3937e-7i$	$2.0947e-4 + 6.6559e-4i$
2	$3.6046e-4 - 1.1859e-4i$	$0.0192 + 0.0303i$
3	$0.0007 + 0.0013i$	$0.0131 - 0.3226i$
4	$-27.8334 + 39.7377i$	$-1.4950e-4 - 9.8894e+3i$
⋮	⋮	⋮
157	$0.000 + 0.000i$	$-5.3637e-5 - 1.1583e-5i$
158	$0.000 + 0.000i$	$-1.2522e-5 - 2.0176e-5i$
159	$0.000 + 0.000i$	$1.7225e-6 + 2.4589e-7i$
160	$0.000 + 0.000i$	$4.7504e-7 - 3.8804e-8i$

TABLE 23 Computation of the right eigenvectors and their derivatives for the eigenvalue λ_{160}.

Reduced DOF	Right eigenvector η	Right eigenvalues derivatives $\partial\eta/\partial q$
1	$0.000 + 0.000i$	$-1.0597e-11 + 2.9517e-12i$
2	$0.000 + 0.000i$	$5.0508e-13 - 1.8455e-13i$
3	$0.000 + 0.000i$	$1.3162e-12 + 7.7910e-13i$
4	$0.000 + 0.000i$	$-2.1074e-12 + 2.3698e-11i$
⋮	⋮	⋮
157	$31.9806 + 0.0000i$	$0.0000 + 0.0000i$
158	$20.6571 + 17.8384i$	$6.5380e-5 + 1.5593e-4i$
159	$-5.7335 + 2.8326i$	$4.5913e-4 - 2.9393e-4i$
160	$1.6087 + 3.8662i$	$-1.8549e-4 - 4.3889e-4i$

TABLE 24 Computation of the left eigenvectors and their derivatives for the eigenvalue λ_{160}.

Reduced DOF	Left eigenvector ξ	Left eigenvalues derivatives $\partial\xi/\partial q$
1	$1.3169 - 0.3392i$	$-2.2006e-4 + 5.7611e-4i$
2	$-5.9896 - 4.3899i$	$0.0110 - 0.0055i$
3	$-9.6333 + 17.1517i$	$0.0182 - 0.0119i$
4	$0.7333 - 1.0901i$	$-0.0005 + 0.0034i$
⋮	⋮	⋮
157	$31.9806 - 0.0000i$	$0.0000 + 0.0000i$
158	$20.6571 + 17.8384i$	$0.0031 - 0.0163i$
159	$-5.7335 + 2.8326i$	$0.0157 - 0.0121i$
160	$1.6087 + 3.8662i$	$-0.0070 - 0.0170i$

the errors associated with the present method are higher than those reported in the method proposed by Wang and Dai,[3] which introduces an additional normalization condition to extend the system of linear equations with nonsingular coefficient matrices in conjunction with the second-order derivatives of the eigenequations. However, these present errors remain within an acceptable range when compared to the method developed by Li et al.,[1] which yields errors of around 1% by introducing a new normalization for the left eigenvector with the second-order derivatives of the eigenequations. Furthermore, it is worth noting that some of the proposed techniques for computing eigensolution sensitivities did not provide information on the accuracy or error of their respective techniques. Examples of such techniques include those proposed by Adhikari and Friswell,[13] Xu and Wu,[2] Xu et al.,[4] Wang and Yang,[6] Wang et al.,[5] and so forth.

In this paper, the verifications of computed results in Examples 3–5 for a large system are challenging to provide due to several reasons. Firstly, the order of the eigensolutions can be shifted during the analysis, making it difficult to control their orders. Secondly, maintaining the order of the eigensolutions proves to be a complex task. Thirdly, certain systems exhibit non-zero derivatives of the eigenvector while the magnitude of the eigenvector (or its element) itself is zero, as outlined in Li et al.[1]

As a consequence, it becomes evident that none of the previously published solutions for the derivatives of eigenvalues and eigenvectors have provided verifications of their methods on large systems.[1–7] However, examples 3–5 clearly demonstrate that the proposed method in this paper can successfully compute the derivatives of eigensolutions for large rotordynamic structures. Notably, this method achieves accurate results without relying on second derivatives of the eigenequations. Furthermore, it is versatile enough to be utilized in both fixed and co-rotating coordinate systems, incorporating the modal superposition (MS) method-based model order reduction technique. Therefore, the method proposed in this paper offers a more efficient and cost-effective approach for computing eigensensitivity.

4 | CONCLUSION

In this paper, a new algorithm has been proposed for computing eigensolution derivatives with distinct and repeated eigenvalues for asymmetric damped systems, specifically focusing on rotordynamic systems. The proposed method eliminates the need for second-order derivatives of the eigensolutions and introduces two significant advancements. First, new normalization conditions for the left and right eigenvectors are introduced ensuring consistency conditions throughout the computational system. Second, the sensitivity problems are solved by employing the chain rule, offering a fresh perspective compared to existing methods that rely on linear combinations of eigenvectors.

The Application of the chain rule for eigensolution sensitivity computation in this paper is unprecedented in the literature, as evident in Figure 1. This positions the developed method as an alternative to previous approaches utilizing the chain rule. In addition, stability is successfully achieved by suggesting justifying Nelson[16] technique on the basis of the new normalization conditions. A key advantage of the present algorithm is its independence from second-order derivatives of the eigenequations, setting it apart from existing methods. This greatly simplifies its implementation in both analytical and numerical programs. Consequently, the developed approach significantly reduces computational complexity and time requirements.

To validate the correctness and effectiveness of the proposed method, five numerical examples are presented demonstrating the computation of eigensolution derivatives in displacement-space and state-space equations for damped rotordynamic systems. Verifications are provided and found to be in reasonable agreement with the approximate method, thereby highlighting the acceptable accuracy of the developed approach compared to some available solutions.

In conclusion, the proposed algorithm presents a major advancement in the field, offering a more efficient and time-saving solution for computing eigensolution derivatives in asymmetric damped systems. Its novel approach utilizing the chain rule and independence from second-order derivatives positions it as a valuable alternative to existing methods.

ACKNOWLEDGMENTS

The support from the National Research Foundation of Korea (NRF) funded by the Korea government (MSIT) (NRF_2019R1A2C2084974) is gratefully acknowledged. Finally, Ty Phuor would like to especially thank his parents, Chhiv Phuor (deceased) and Ky Hai, his wife, Louchsolida Yin, and his son, Sophearith Phuor, who have provided great support to this work.

CONFLICT OF INTEREST STATEMENT

All authors declare that they have no conflicts of interest.

DATA AVAILABILITY STATEMENT

The datasets generated and/or analyzed the present study are available from the corresponding author upon reasonable request, for instance, the Matlab. FIG, the Matlab. Mat.

ORCID

Ty Phuor https://orcid.org/0000-0002-7909-1974

REFERENCES

1. Li L, Hu Y, Wang X. A parallel way for computing eigenvector sensitivity of asymmetric damped systems with distinct and repeated eigenvalues. *Mech Syst Signal Process*. 2012;30:30-77. doi:10.1016/j.ymssp.2012.01.008
2. Xu Z, Wu B. Derivatives of complex eigenvectors with distinct and repeated eigenvalues. *Int J Numer Methods Eng*. 2008;75(8):945-963. doi:10.1002/nme.2280
3. Wang P, Dai H. Calculation of eigenpair derivatives for asymmetric damped systems with distinct and repeated eigenvalues. *Int J Numer Methods Eng*. 2015;103(7):501-515. doi:10.1002/nme.4901
4. Xu ZH, Zhong HX, Zhu XW, Wu BS. An efficient algebraic method for computing eigensolution sensitivity of asymmetric damped systems. *J Sound Vib*. 2009;327(3–5):584-592. doi:10.1016/j.jsv.2009.07.013
5. Wang P, Wu J, Yang X. An improved method for computing Eigenpair derivatives of damped system. *Math Probl Eng*. 2018;2018:1-8. doi:10.1155/2018/8050132
6. Wang P, Yang X. Eigensensitivity of damped system with defective multiple eigenvalues. *J Vibroeng*. 2016;18(4):2331-2342. doi:10.21595/jve.2016.15791
7. Wang P, Yang X, Mi J. Computing eigenpair derivatives of asymmetric damped system by generalized inverse. *J Vibroeng*. 2017;19(7):5290-5300. doi:10.21595/jve.2017.18232
8. Fox RL, Kapoor MP. Rates of change of eigenvalues and eigenvectors. *AIAA J*. 1968;6(12):2426-2429. doi:10.2514/3.5008
9. Rogers LC. Derivatives of eigenvalues and eigenvectors. *AIAA J*. 1970;8(5):943-944. doi:10.2514/3.5795
10. Plaut RH, Huseyin K. Derivatives of eigenvalues and eigenvectors in non-self-adjoint systems. *AIAA J*. 1973;11(2):250-251. doi:10.2514/3.6740
11. Adhikari S. Rates of change of eigenvalues and eigenvectors in damped dynamic system. *AIAA J*. 1999;37(11):1452-1458. doi:10.2514/2.622
12. Adhikari S. Calculation of derivative of complex modes using classical normal modes. *Comput Struct*. 2000;77(6):625-633. doi:10.1016/S0045-7949(00)00016-X
13. Adhikari S, Friswell MI. Eigenderivative analysis of asymmetric non-conservative systems. *Int J Numer Methods Eng*. 2001;51(6):709-733. doi:10.1002/nme.186.abs
14. Zeng QH. Highly accurate modal method for calculating eigenvector derivatives in viscous damping systems. *AIAA J*. 1995;33(4):746-751. doi:10.2514/3.12453
15. Moon YJ, Kim BW, Ko MG, Lee IW. Modified modal methods for calculating eigenpair sensitivity of asymmetric damped system. *Int J Numer Methods Eng*. 2004;60(11):1847-1860. doi:10.1002/nme.1025
16. Nelson RB. Simplified calculation of eigenvector derivatives. *AIAA J*. 1976;14(9):1201-1205. doi:10.2514/3.7211
17. Mills-Curran WC. Calculation of eigenvector derivatives for structures with repeated eigenvalues. *AIAA J*. 1988;26(7):867-871. doi:10.2514/3.9980

18. Ojalvo IU. Efficient computation of modal sensitivities for systems with repeated frequencies. *AIAA J*. 1988;26(3):361-366. doi:10.2514/3.9897
19. Dailey RL. Eigenvector derivatives with repeated eigenvalues. *AIAA J*. 1989;27(4):486-491. doi:10.2514/3.10137
20. Shaw J, Jayasuriya S. Modal sensitivities for repeated eigenvalues and eigenvalue derivatives. *AIAA J*. 1992;30(3):850-852. doi:10.2514/3.10999
21. Tang J, Ni WM, Wang WL. Eigensolutions sensitivity for quadratic eigenproblems. *J Sound Vib*. 1996;196(2):179-188. doi:10.1006/jsvi.1996.0475
22. Tang J, Wang WL. On calculation of sensitivity for non-defective eigenproblems with repeated roots. *J Sound Vib*. 1999;225(4):611-631. doi:10.1006/jsvi.1999.2098
23. Friswell MI, Adhikari S. Derivatives of complex eigenvectors using Nelson's method. *AIAA J*. 2000;38(12):2355-2357. doi:10.2514/2.907
24. Lee IW, Jung GH, Lee JW. Numerical method for sensitivity analysis of eigensystems with non-repeated and repeated eigenvalues. *J Sound Vib*. 1996;195(1):17-32. doi:10.1006/jsvi.1996.9989
25. Burchett BT, Costello M. QR-based algorithm for eigenvalue derivatives. *AIAA J*. 2002;40(11):2319-2322. doi:10.2514/2.1569
26. Xie H, Dai H. Davidson method for eigenpairs and their partial derivatives of generalized eigenvalue problems. *Commun Numer Methods Eng*. 2006;22(2):155-165. doi:10.1002/cnm.811
27. Lee TH. Adjoint method for design sensitivity analysis of multiple eigenvalues and associated eigenvectors. *AIAA J*. 2007;45(8):1998-2004. doi:10.2514/1.25347
28. Burchett BT. QZ-based algorithm for system pole, transmission zero, and residue derivatives. *AIAA J*. 2009;47(8):1889-1901. doi:10.2514/1.39759
29. Yoon GH, Donoso A, Carlos Bellido J, Ruiz D. Highly efficient general method for sensitivity analysis of eigenvectors with repeated eigenvalues without passing through adjacent eigenvectors. *Int J Numer Methods Eng*. 2020;121(20):4473-4492. doi:10.1002/nme.6442
30. Garg S. Derivatives of eigensolutions for a general matrix. *AIAA J*. 1973;11(8):1191-1194. doi:10.2514/3.6892
31. Rudisill CS. Derivatives of eigenvalues and eigenvectors for a general matrix. *AIAA J*. 1974;12(5):721-722. doi:10.2514/3.49330
32. Rudisill CS, Chu YY. Numerical methods for evaluating the derivatives of eigenvalues and eigenvectors. *AIAA J*. 1975;13(6):834-837. doi:10.2514/3.60449
33. Lee IW, Jung GH. An efficient algebraic method for the computation of natural frequency and mode shape sensitivities–Part I. Distinct natural frequencies. *Comput Struct*. 1997;62(3):429-435. doi:10.1016/S0045-7949(96)00206-4
34. Lee IW, Jung GH. An efficient algebraic method for the computation of natural frequency and mode shape sensitivities–Part II. Multiple natural frequencies. *Comput Struct*. 1997;62(3):437-443. doi:10.1016/S0045-7949(96)00207-6
35. Choi KM, Cho SW, Ko MG, Lee IW. Higher order eigensensitivity analysis of damped systems with repeated eigenvalues. *Comput Struct*. 2004;82(1):63-69. doi:10.1016/j.compstruc.2003.08.001
36. Lee IW, Kim DO, Jung GH. Natural frequency and mode shape sensitivities of damped systems: part I, distinct natural frequencies. *J Sound Vib*. 1999;223(3):399-412. doi:10.1006/jsvi.1998.2129
37. Wu B, Xu Z, Li Z. A note on computing eigenvector derivatives with distinct and repeated eigenvalues. *Commun Numer Methods Eng*. 2007;23(3):241-251. doi:10.1002/cnm.895
38. Guedria N, Smaoui H, Chouchane M. A direct algebraic method for eigensolution sensitivity computation of damped asymmetric systems. *Int J Numer Methods Eng*. 2006;68(6):674-689. doi:10.1002/nme.1732
39. Chouchane M, Guedria N, Smaoui H. Eigensensitivity computation of asymmetric damped systems using an algebraic approach. *Mech Syst Signal Process*. 2007;21(7):2761-2776. doi:10.1016/j.ymssp.2007.01.007
40. Phuor T, Yoon GH. Model order reduction for Campbell diagram analysis of shaft-disc-blade system in 3D finite elements. *Struct Eng Mech*. 2022;81(4):411-428. doi:10.12989/sem.2022.81.4.411
41. Phuor T. Development and application of three-dimensional finite element interface model for soil-jack-up interaction during preloading [PhD Thesis]. 2020.
42. Phuor T, Harahap ISH, Ng CY, Al-Bared MA. Development of the skew boundary condition for soil-structure interaction in three-dimensional finite element analysis. *Comput Geotech*. 2021;137:104264. doi:10.1016/j.compgeo.2021.104264
43. Phuor T, Harahap ISH, Ng CY. Bearing capacity factors for rough conical footing by viscoplasticity finite element analysis. *ASCE Int J Geomech*. 2021;22(1):04021266. doi:10.1061/(ASCE)GM.1943-5622.0002256
44. Phuor T, Harahap IS, Ng C-Y. Bearing capacity factors of flat base footing by finite elements. *ASCE J Geotech Geoenviron Eng*. 2022;148(8):04022062. doi:10.1061/(ASCE)GT.1943-5606.0002835
45. Phuor T, Ganz A, Trapper PA. Bearing capacity factors of the cone-shaped footing in meshfree. *Int J Numer Anal Methods Geomech*. 2022;47:275-298. doi:10.1002/nag.3469
46. Strauß F, Inagaki M, Starke J. Reduction of vibration level in rotordynamics by design optimization. *Struct Multidiscip Optim*. 2007;34(2):139-149. doi:10.1007/s00158-006-0065-3
47. Nelson HD, McVaugh JM. The dynamics of rotor-bearing systems using finite elements. *J Manuf Sci E T ASME*. 1976;98:593-600. doi:10.1115/1.3438942
48. Nelson HD. A finite rotating shaft element using Timoshenko beam theory. *J Mech Des Trans ASME*. 1980;102:793-803. doi:10.1115/1.3254824
49. Nandi A, Neogy S. Modelling of rotors with three-dimensional solid finite elements. *J Strain Anal Eng Des*. 2001;6(4):359-371. doi:10.1243/0309324011514539

50. Rahman T, Valdman J. Fast MATLAB assembly of FEM matrices in 2D and 3D: nodal elements. *Appl Math Comput*. 2013;219(13):7151-7158. doi:10.1016/j.amc.2011.08.043

SUPPORTING INFORMATION

Additional supporting information can be found online in the Supporting Information section at the end of this article.

How to cite this article: Phuor T, Yoon GH. Eigensensitivity of damped system with distinct and repeated eigenvalues by chain rule. *Int J Numer Methods Eng*. 2023;124(21):4687-4717. doi: 10.1002/nme.7331

APPENDIX A. FOR EXAMPLE 3

- The lagrangian equation of motion of the rigid disk with the constant speed restriction (Ω) in the fixed reference system can be written as[47]

$$\left(\left[M_T^d\right]+\left[M_R^d\right]\right)\left\{\ddot{q}^d\right\}-\Omega\left[G^d\right]\left\{\dot{q}^d\right\}=\left\{Q^d\right\}$$

where,

$$\left[M_T^d\right]=\begin{bmatrix} m_d & 0 & 0 & 0\\ 0 & m_d & 0 & 0\\ 0 & 0 & 0 & 0\\ 0 & 0 & 0 & 0\end{bmatrix},\left[M_R^d\right]=\begin{bmatrix} 0 & 0 & 0 & 0\\ 0 & 0 & 0 & 0\\ 0 & 0 & I_d & 0\\ 0 & 0 & 0 & I_d\end{bmatrix},\left[G^d\right]=\begin{bmatrix} 0 & 0 & 0 & 0\\ 0 & 0 & 0 & 0\\ 0 & 0 & 0 & I_p\\ 0 & 0 & I_p & 0\end{bmatrix}$$

$$\left[\widehat{M}_T^d\right]=\begin{bmatrix} 0 & -m_d & 0 & 0\\ m_d & 0 & 0 & 0\\ 0 & 0 & 0 & 0\\ 0 & 0 & 0 & 0\end{bmatrix},\left[\widehat{M}_R^d\right]=\begin{bmatrix} 0 & 0 & 0 & 0\\ 0 & 0 & 0 & 0\\ 0 & 0 & 0 & -I_d\\ 0 & 0 & I_d & 0\end{bmatrix},\left[\widehat{G}^d\right]=\begin{bmatrix} 0 & 0 & 0 & 0\\ 0 & 0 & 0 & 0\\ 0 & 0 & -I_p & 0\\ 0 & 0 & 0 & -I_p\end{bmatrix}$$

where, m_d is the disk mass, I_d is the disk diametral inertia, $\left\{Q^d\right\}$ is the external force vector, and I_P is the disk polar inertia.

- The lagrangian equation of motion for the finite rotor element with the constant spin speed restriction (Ω) in the fixed body system can be expressed as[47]

$$\left(\left[M_T^e\right]+\left[M_R^e\right]\right)\left\{\ddot{q}^e\right\}-\Omega\left[G^e\right]\left\{\dot{q}^e\right\}+\left[K_B^e\right]\left\{q^e\right\}=\left\{Q^e\right\}$$

where,

$$\left[M_T^e\right]=\frac{\mu l}{420}\begin{bmatrix} 156 & 0 & 0 & 22l & 54 & 0 & 0 & -13l\\ 0 & 156 & -22l & 0 & 0 & 54 & 13l & 0\\ 0 & -22l & 4l^2 & 0 & 0 & -13l & -3l^2 & 0\\ 22l & 0 & 0 & 4l^2 & 13l & 0 & 0 & -3l^2\\ 54 & 0 & 0 & 13l & 156 & 0 & 0 & -22l\\ 0 & 54 & -13l & 0 & 0 & 156 & 22l & 0\\ 0 & 13l & -3l^2 & 0 & 0 & 22l & 4l^2 & 0\\ -13l & 0 & 0 & -3l^2 & -22l & 0 & 0 & 4l^2\end{bmatrix}$$

$$\left[M_R^e\right] = \frac{\mu r^2}{120l}\begin{bmatrix} 36 & 0 & 0 & 3l & -36 & 0 & 0 & 3l \\ 0 & 36 & -3l & 0 & 0 & -36 & -3l & 0 \\ 0 & -3l & 4l^2 & 0 & 0 & 3l & -l^2 & 0 \\ 3l & 0 & 0 & 4l^2 & -3l & 0 & 0 & -l^2 \\ -36 & 0 & 0 & -3l & 36 & 0 & 0 & -3l \\ 0 & -36 & 3l & 0 & 0 & 36 & 3l & 0 \\ 0 & -3l & -l^2 & 0 & 0 & 3l & 4l^2 & 0 \\ 3l & 0 & 0 & -l^2 & -3l & 0 & 0 & 4l^2 \end{bmatrix}$$

$$\left[G^e\right] = \frac{2\mu r^2}{120l}\begin{bmatrix} 0 & 36 & -3l & 0 & 0 & -36 & -3l & 0 \\ 36 & 0 & 0 & -3l & 36 & 0 & 0 & -3l \\ -3l & 0 & 0 & 4l^2 & -3l & 0 & 0 & -l^2 \\ 0 & -3l & 4l^2 & 0 & 0 & -3l & l^2 & 0 \\ 0 & 36 & -3l & 0 & 0 & 36 & 3l & 0 \\ -36 & 0 & 0 & -3l & 36 & 0 & 0 & 3l \\ -3l & 0 & 0 & l^2 & 3l & 0 & 0 & 4l^2 \\ 0 & -3l & -l^2 & 0 & 0 & 3l & 4l^2 & 0 \end{bmatrix}$$

$$\left[K_B^e\right] = \frac{EI}{l^3}\begin{bmatrix} 12 & 0 & 0 & 6l & -12 & 0 & 0 & 6l \\ 0 & 12 & -6l & 0 & 0 & 12 & -6l & 0 \\ 0 & -6l & 4l^2 & 0 & 0 & 6l & 2l^2 & 0 \\ 6l & 0 & 0 & 4l^2 & -6l & 0 & 0 & 2l^2 \\ -12 & 0 & 0 & -6l & 12 & 0 & 0 & -6l \\ 0 & 12 & 6l & 0 & 0 & 12 & 6l & 0 \\ 0 & -6l & 2l^2 & 0 & 0 & 6l & 4l^2 & 0 \\ 6l & 0 & 0 & 2l^2 & -6l & 0 & 0 & 4l^2 \end{bmatrix}$$

$$\left[\widehat{M}_T^e\right] = \frac{\mu l}{420}\begin{bmatrix} 0 & 156 & -22l & 0 & 0 & 54 & 13l & 0 \\ 156 & 0 & 0 & -22l & -54 & 0 & 0 & -13l \\ -22l & 0 & 0 & 4l^2 & 13l & 0 & 0 & -3l^2 \\ 0 & -22l & 4l^2 & 0 & 0 & -13l & 3l^2 & 0 \\ 0 & -54 & 13l & 0 & 0 & 156 & 22l & 0 \\ 54 & 0 & 0 & -13l & 156 & 0 & 0 & -22l \\ 13l & 0 & 0 & 3l^2 & 22l & 0 & 0 & 4l^2 \\ 0 & -13l & -3l^2 & 0 & 0 & -22l & 4l^2 & 0 \end{bmatrix}$$

where, μ is the element mass per unit length, l is the length of the shaft, $\{Q^e\}$ is the external force vector, and r is here the radius of the shaft.

APPENDIX B. FOR EXAMPLES 4 AND 5

- The general equation of motion of the rotating structure with the constant speed restriction (Ω) in the co-rotating reference system in three-dimensional finite element analysis can be written as[40,49]

$$M \cdot \ddot{r}(t) + [C_d + C_c(\Omega) + C_b(\Omega)] \cdot \dot{r}(t) + [K_e + K_c(\Omega) - K_s(\Omega) + K_b(\Omega)] \cdot r(t) = f(t)$$

where,

$$M = \iiint_{V_e} [N]^T [N] \rho \cdot dV_e$$

$$C_c(\Omega) = 2\Omega \iiint_{V_e} [N_1]^T \begin{bmatrix} 0 & -1 \\ 1 & 0 \end{bmatrix} [N_1] \rho \cdot dV_e$$

$$[K_e] = \iiint_{V_e} [B]^T \cdot [D] \cdot [B] \cdot dV_e$$

$$[K_s(\Omega)] = \Omega^2 \iiint_{V_e} [N_1]^T [N_1] \rho \cdot dV_e$$

$$[K_c(\Omega)] = \Omega^2 \iiint_{V_e} [N_2]^T [N_2] \rho \cdot dV_e$$

$K_b(\Omega)$ and $C_b(\Omega)$ are respectively the stiffness and damping matrices induced by the bearing system. f(t) and C_d are the external force vector and the structural damping, respectively. $r(t), \dot{r}(t)$ and $\ddot{r}(t)$ respectively denotes the vector of displacement, velocity and acceleration responses of the rotordynamic system.